A novel model evaluation approach focussing on local and advected contributions to urban $PM_{2.5}$ levels – Application to Paris, France

H. Petetin[1], M. Beekmann[1], J. Sciare[2], M. Bressi[2], A. Rosso[3], O. Sanchez[3], V. Ghersi[3]

(1) {LISA/IPSL, Laboratoire Interuniversitaire des Systèmes Atmosphériques, UMR CNRS 7583, Université Paris Est Créteil (UPEC) et Université Paris Diderot (UPD), France.}

(2) {LSCE, Laboratoire des Sciences du Climat et de l'Environnement, CNRS-CEA-UVSQ, Gif-sur-Yvette, France}

(3) {AIRPARIF, Agence de surveillance de la qualité de l'air, Paris, France}

Correspondence to: H. Petetin (herve.petetin@lisa.u-pec.fr)

Abstract

Aerosol simulations in chemistry transport models (CTMs) still suffer from numerous uncertainties, and diagnostic evaluations are required to point out major error sources. This paper presents an original approach to evaluate CTMs based on local and imported contributions in a large megacity rather than urban background concentrations. The study is applied to the CHIMERE model in the Paris region (France) and considers the fine particulate matter ($PM_{2.5}$) and its main chemical constituents (elemental and organic carbon, nitrate, sulfate and ammonium), for which daily measurements are available during a whole year at various stations (PARTICULES project). Back-trajectory data are used to locate the upwind station, from which the concentration is identified as the import, the local production being deduced from the urban concentration by subtraction. Uncertainties on these contributions are quantified. Small biases in urban background $PM_{2.5}$ simulations (bias of +16%) hide significant error compensations between local and advected contributions, as well as in $PM_{2.5}$ chemical compounds. In particular, wintertime OM imports appear strongly underestimated while local OM and EC production are overestimated all along the year. Erroneous continental woodburning emissions and missing SOA pathways may explain errors on advected OM, while carbonaceous compounds overestimation is likely to be related to errors in emissions and

dynamics. A statistically significant local formation of nitrate is also highlighted from observations, but missed by the model. Together with the overestimation of nitrate imports, it leads to a bias of +51% on the local $PM_{2.5}$ contribution. Such an evaluation finally gives more detailed insights on major gaps in current CTMs on which future efforts are needed.

1 Introduction

Fine particulate matter ($PM_{2.5}$, particulate matter with aerodynamic diameter below 2.5 μm) pollution is well-known to produce adverse health effects (Chow et al., 2006), and to affect ecosystems and monuments through acidic deposition soiling (Likens et al., 1996; Lombardo et al., 2013). It also impacts on climate directly through its diffusing and absorptive properties and indirectly through various modifications of cloud properties (Lohmann and Feichter, 2005), leading to changes in the earth radiative balance (Forster et al., 2007).

In the European Union, many member states, including France, still fail to reach both daily and annual PM standards (EEA, 2012). Besides some rural areas (e.g. Po valley and Silesia), the exceedences of air quality standards mainly occur in cities that gather population and associated anthropogenic activities. In 2010, about 21% of EU urban population has been exposed to levels not complying with the PM_{10} daily limit value (daily 50 μg m^{-3} concentration exceeded less than 35 days per year). During the 2001-2010 period, all regulated EU pollutant emissions contributing to fine particles have decreased: by about -15% for $PM_{2.5}$ (decrease in all source sectors except non-industrial fuel combustion that increases), and for its gaseous precursors by about -54% for SO_2, -27% for NO_x, and -10% for NH_3. Nevertheless, trends in $PM_{2.5}$ concentrations remain unclear (EEA, 2012), due to variations in meteorological conditions and due to the possibly important contribution of biogenic sources.

Chemistry-transport models (CTMs) have become a very useful tool for both air quality forecasting and emission scenario analysis in order to help air quality managers and policy-makers finding appropriate solutions for pollution abatement. Nevertheless, strong uncertainties in emissions, meteorological data, physical parametrisations and chemical schemes still prevent CTMs to correctly retrieve PM concentrations and even more its chemical speciation. In the framework of the Air Quality Modelling Evaluation International Initiative (AQMEII) project (Rao et al., 2011), a recent cross-comparison over a whole year of ten CTMs in Europe and North America has shown a strong variability between models, with root-mean square errors (RMSE) for PM_{10} around 7.3-15.2 μg m^{-3} (Solazzo et al., 2012). Most of these models tend to largely underestimate PM_{10} concentrations, with biases ranging from -14 to +1.4 μg m^{-3}.

Results are better for $PM_{2.5}$, particularly in terms of correlation (R in the range of 0.4-0.8, compared to 0.2-0.7 for PM_{10}). Authors have underlined that performances and discrepancies between models are also important during specific episodes of enhanced PM levels. By comparing five CTMs during a winter PM episode in Europe, Stern et al. (2008) has shown biases ranging from -15 to +7 $\mu g\ m^{-3}$. Many other model studies in Europe (e.g. Sartelet et al., 2007) drew similar conclusions concerning the PM underestimation.

Various uncertainty sources are at stake in CTMs. Among them, emissions still remain a critical point, with strong uncertainties both in emission factors and/or spatial distribution for some source sectors, such as biomass burning, road dust re-suspension (usually missing in inventories), agriculture. Even with similar input data, discrepancies can raise from emission preprocessing (Solazzo et al., 2012). Secondary organic aerosol (SOA) formation also represents a large field of research, with various formation pathways still ignored or poorly understood (see for example Hallquist et al., 2009 and references therein). Meteorological errors can also impact on PM levels through advection and dispersion (wind speed and direction, vertical mixing in the boundary layer) or removal by precipitation (Vautard et al., 2012). In their cross-comparison, Solazzo et al. (2012) have underlined that underestimated wind speed and overestimated precipitation frequency can partly explain the negative PM_{10} bias. Because of the lack of measurements, dry deposition represents another important uncertainty source (Nopmongcol et al. 2012).

CTM evaluation is traditionally limited to comparison between modelled and measured concentrations at various sites. Nevertheless, such an approach usually conceals the geographic provenance of errors in terms of local emission/production and regional import. This is particularly important for $PM_{2.5}$ since, in addition to direct emissions, it can be formed from gaseous precursors and advected over long distances, due to limited chemical removal pathways for most of PM compounds and slow dry deposition of aerosol present in the accumulation mode (Van Dingenen et al., 2004). This sometimes leads to strong regional background that is advected toward cities and adds to the local urban pollution increment. Large advected PM contributions have already been shown in megacities such as New York through strong proportions of secondary species, with 54 and 24% of organic aerosol (mainly oxidized, at 64%) and sulfate respectively (Sun et al., 2011). Several studies in Paris have indicated the potential significant influence of PM imports (Sciare et al., 2010; Bressi et al., 2013, Zhang et al., 2013). Through a modeling exercice of long-term PM_{10} concentrations in

the Paris region, Hodzic et al. (2005) have pointed out some error compensations between the local production and the rural background.

If many PM studies in megacities have recently given rise to a potential strong advected contribution, very few have intended to systematically quantify it. Lenschow et al. (2001) have developed a methodology (that will be detailed in Sect. 4), based on measurements at sites of various typology (rural and urban background, traffic) and applied to the Greater Berlin area, to discriminate these local and regional contributions. This approach turns out to be useful in air quality management to assess both the sources of $PM_{2.5}$ and the relevance to work on local emissions. Results have shown that the long-range transport accounts for about 50% of the Berlin urban background PM_{10} concentrations.

Based on this approach, this paper intends to evaluate the ability of a regional CTM to retrieve the correct share between local and imported $PM_{2.5}$ contributions in a large megacity. Assessing these two contributions separately is a novel and useful approach which goes beyond traditional model evaluation based on simulation-observation comparisons for particular sites. It will be applied to the CHIMERE model in the Greater Paris region. This large urban area gathers all the characteristics of a megacity, including more than 10 million inhabitants and concentrates an important part of the French economic activities.

The observational data base used in this paper is based on the results of the one year PARTICULES campaign (AIRPARIF, 2012, Bressi et al. 2013) in the Greater Paris region, that consists in daily $PM_{2.5}$ chemical speciation measurements at various sites.

After a short description of the measurement data base (Sect. 2), the CHIMERE model will be presented as well as its configuration used for this study (Sect. 3). Then the methodology to derive the urban and the advected part of $PM_{2.5}$ will be detailed (Sect. 4). Results will be first analysed for each of the main $PM_{2.5}$ compounds and then implications for model evaluation will be discussed (Sect. 5), before conclusion (Sect. 6).

2 Measurement data base

In the framework of the PARTICULES project (AIRPARIF-LSCE), daily (from 00:00 to 23:59 LT) $PM_{2.5}$ chemical mass closure measurements have been performed in the Paris region and its surroundings during a whole year period, from the 11 September 2009 to the 10 September 2010. Six sites have been documented, including an urban background site (PAR) and three rural background sites, respectively in the north-east (RNE), south (RUS) and north-west

(RNW) of Paris. Bressi et al. (2013) have described in details the sampling and analytical setup and have presented the experimental database obtained from this campaign. At each site, $PM_{2.5}$ have been collected by two Leckel samplers, one equipped with Teflon filters for gravimetric and ions measurements, the other with quartz filters for carbon measurements. Measurement techniques and uncertainty estimates for main compounds are summarized in Table 1.

Three different measurements of $PM_{2.5}$ concentration are available (among which two are independent): the $PM_{2.5}$ concentration measured by TEOM-FDMS considered here as reference (PM_{ref}), the gravimetric measurement at RH below 20% (PM_{grav}), and the chemically reconstructed $PM_{2.5}$ concentration calculated from the aforementioned measurements/estimations of each compound (PM_{chem}). That last value requires OC measurements to be converted into organic matter (OM). The OM/OC conversion factors are taken as 1.95 and 2.05 for the urban and the rural background sites respectively, in general agreement although in the upper range of values given by other studies (Bressi et al., 2013). Using only these conversion factors, correlation coefficients (R^2) between PM_{chem} and PM_{grav} reach more than 0.98 at every site. In order to be consistent with the chemical compounds analysis, notably in terms of contribution, all $PM_{2.5}$ concentrations mentioned in the paper refer to PM_{grav} measurements.

It is worthwhile noting that filter sampling can induce significant artefacts especially due to evaporation of volatile compounds (mainly ammonium nitrate and organic species) (Pang et al., 2002), or adsorption and eventually oxidation of some gaseous compounds (such as nitric acid, ammonia, sulfur dioxide or some volatile organic carbons, VOC) (Cheng and Tsai, 1997; and references therein). To assess the uncertainties associated with these filter measurements, Bressi et al. (2013) have performed an intercomparison during 40 days in wintertime for ion measurements with a particle-into-liquid-sampler (PILS) coupled with ion chromatography (IC). A satisfactory agreement has been found, with discrepancies remaining in the range of the measurement uncertainty fixed by the authors, i.e. around 20%. Another intercomparison has been performed for carbonaceous compounds during 70 days in winter and early spring with hourly VOC denuded EC and OC concentrations from OCEC Sunset field instrument, again leading to satisfactory agreement (discrepancies below 25%, i.e. in the range of measurement uncertainties). However, these comparisons have been carried out during a period with potentially low evaporation (low temperature, high RH), whereas various studies have shown that filter measurement artefacts increase with higher temperature (Keck et al., 2005; Yu et al., 2006).

Based on TEOM-FDMS measurements (PM_{ref}) available during the campaign, it is possible to derive an upper limit of the error induced by filter measurements. The comparison with PM_{grav} shows that filter artefacts are mostly negative, meaning that evaporation losses on filter exceed adsorption gains (except in August). By assuming that this error mainly affects ammonium nitrate and organic matter, one can estimate the underestimation of the total of both compounds at around -30% in winter and -50% in summer (see analysis in the Supplement, Sect. S.1).

Concerning EC, it is to be noted that differences with black carbon (BC) measurements (Andreae et Gelencsér, 2006; Salako, 2012) can lead to misinterpretations of comparisons with model results if emission factors used in the inventory are not consistent with the measurements. In our case, the PM speciation used in simulations is derived from EC (and not BC) emission factors.

This study will focus on the main $PM_{2.5}$ components analysed during the PARTICULES campaign: OM, EC, nitrate, sulfate and ammonium. Sea salts and dust were minor compounds, and are not directly used for model evaluation. Note that for $PM_{2.5}$ and these six chemical constituents, depending on the station, the missing data percentage ranges between 2 and 10% of the year.

3 Simulations

3.1 CHIMERE model

Our work in this paper is performed with the v2008b version of the CHIMERE regional CTM (Schmidt et al. 2001; Bessagnet et al., 2009; Menut et al. 2013) (www.lmd.polytechnique.fr/chimere). This model is widely used both in research activities and operational air pollution survey and forecasting in France (ESMERALDA, www.esmeralda-web.fr, and PREVAIR, www.prevair.org, platforms run by AIRPARIF for North and West of France and by PREVAIR at the national scale respectively) and European Union (GMES-MACC program). The ESMERALDA project is a pooling of technical, human and financial means for Air quality forecast system and emission inventory set-up by 9 French air quality monitoring networks, Atmo Picardie, Atmo Nord-Pas de Calais (North of France), Atmo Champagne-Ardennes, LIG'AIR (Centre region), Air Normand (Haute-Normandie), AIRPARIF (Ile de France), ATMOSF'AIR (Burgundy), AIRCOM (Basse-Normandie), AIR

BREIZH (Brittany). In the following, a focus will be made on the aerosol module of the CHIMERE model, which is of particular interest for this study.

3.2 Aerosol module description

The main processes affecting the aerosol size distribution and chemical speciation are represented in the CHIMERE aerosol module. This includes emissions, nucleation, coagulation, condensation, and dry and wet deposition. Through a sectional representation within 8 bins of size (diameter ranging from about 40 nm to 10 μm), the module takes into account various chemical species: primary material — including primary organic aerosol (POA), EC and the so-called mineral particulate matter (MPM) corresponding to the remaining part —, nitrate, sulfate, ammonium, water and SOA compounds.

Primary species (POA, EC, MPM) are treated as inert species than can only deposit by wet and/or dry processes. The SOA scheme consists in a single-step oxidation of anthropogenic and biogenic VOC lumped species, giving directly semi-volatile organic compounds that partition between gaseous and particulate phases. SOA yields come from laboratory experiments (Pun and Seigneur, 2007). SOA precursors include fives biogenic lumped species — API (alpha-pinene, sabinene), BPI (beta-pinene, delta-3-carene), LIM (limonene), OCI (ocimene, myrcene), ISO (isoprene) — and three anthropogenic ones — TOL (benzene, toluene, other mono-substituted aromatics), TMB (trimethylbenzene, other poly-substituted aromatics) and n-C_4H_{10} (higher alkanes).

Absorption processes are considered using a kinetical-dynamical approach, with equilibrium concentrations derived from a tabulated version of the ISORROPIA thermodynamic model (Nenes et al, 1998) for secondary inorganic species, and from a temperature dependent partition coefficient according to Pankow (1994) for semi-volatile organic species. Coagulation (Gelbart and Seinfeld, 1980) and sulfuric acid nucleation (Kulmala et al., 1998) are also included in the model.

Aqueous sulfate chemistry is represented (Lee and Schwartz, 1983; Berge, 1993), including iron and manganese catalyzed oxidation reactions of the sulfite ion (SO_3^{2-}) and hydrogen sulfite (HSO_3^-) (Hoffman and Calvert, 1985). Some heterogeneous reactions recommended by Jacob (2000) are also included in the model to take into account the nitric acid formation onto existing particles and cloud droplets. Additionally, the HONO production from NO_2 reactions on wet particles (Aumont et al., 2003) is added.

The dry deposition parametrisation follows the traditional resistance analogy (Wesely, 1989). Concerning wet deposition, the model accounts for both in-cloud (Tsyro, 2002 ; Guelle et al., 1998) and sub-cloud wet scavenging.

3.3 Model configuration

Simulations are performed with the ESMERALDA operational modelling platform. Three nested domains — a large (LAR), a medium (MED) and a fine (FIN) one — are considered with horizontal resolution progressively increasing from 0.5° (roughly 50 km) to 15 km to 3 km (see Fig. 1 and description in Table 2), each with eight vertical levels, from 40 m to about 5 km height.

Meteorological inputs come from PSU/NCAR MM5 simulations (Dudhia, 1993), performed over three nested domains with increasing resolutions of 45, 15 and 5 km respectively, and using Final Analyses (FNL) data from National Centers for Environmental Prediction (NCEP) as boundary conditions and large scale data.

Anthropogenic emissions come from the 1x1km-resolved local ESMERALDA inventory developed by local agencies over the so-called ESM area (delimited by administrative borders, see Fig. 1), e.g. AIRPARIF (2010) for the Paris region and mainly derived from a bottom-up approach. Following the methodology developed in the European FP7/HEAVEN project, traffic emissions are computed from traffic data, fleet description and emission factors using the COPERT IV approach (EEA, 2013). Fuel evaporation emissions are also taken into account. However, road, tire and brake abrasion emissions are ignored, as well as road dust re-suspension. So far, ammonia traffic emissions are not taken into account. The inventory includes emissions from other means of transport (aircraft, shipping, railway). Industrial sector emissions are derived from official statements when they exist or are computed from various types of data (e.g. national raw material consumptions, national productions). Basically, residential emissions are mostly computed using a bottom-up approach, from detailed housing local data (fuel type, housing type, age and size) and associated national consumption estimates. For wood burning related residential emissions, because of the lack of local data, equipment (boiler, open/closed fireplaces, etc.) distribution is taken from national statistics. These ESMERALDA emissions are applied to both the MED and FIN domains, while emissions outside the ESM area are taken from the 0.5x0.5°-resolved EMEP inventory for all primary pollutants (Vestreng et al., 2007). Note that only this last inventory is used in the coarse simulation over the LAR domain.

Biogenic emissions (including isoprene, alpha- and beta-pinene, limonene, ocimene, humulene) are computed from MEGAN emission factors (Guenther et al., 2006), apart from the ESM area where refined biogenic emission factors are computed from the 1x1km-resolved French national forest inventory (NFI). The landuse data used to process emissions is taken from Corine Land Cover (EEA, 2000), with a resolution of 250 m over Europe. Table S1 in Supplement (Sect. S.2) gives the speciations of $PM_{2.5}$ into EC, OM, and mineral PM used for both the continental domain (with EMEP emissions) and the two refined domains (with the ESMERALDA inventory). For these latter domains, speciation is based on a bibliographic study carried out by AIRPARIF. Initial and boundary conditions are taken from LMDz-INCA2 (Folberth et al., 2006) global model for gaseous species and GOCART (Chin et al., 2000) for particulate species.

4 Methodology

4.1 Determination of the advected and local $PM_{2.5}$ fraction

The local Greater Paris urban contribution to $PM_{2.5}$ levels can be deduced from concentrations measured at rural and urban background sites following the so-called Lenschow approach (Lenschow et al., 2001). Daily PM measurements are available at one urban (PAR (48.849°N, 2.365°E)) and three rural background sites located in three directions (RNE (49.088°N, 3.076°E), RUS (48.363°N, 2.26°E), RNW (49.063°N, 1.866°E)). Such a data set allows discriminating the local contribution to urban $PM_{2.5}$ levels by subtracting the appropriate upwind rural concentration. To choose the upwind site among the three rural background sites, a rather simple and automatic procedure has been developed, based on back-trajectories. During the whole year, the FLEXTRA model (Stohl et al., 2001) has been initiated each 6 hours with 10 particles distributed in the center of Paris, leading to a daily set of 40 back-trajectories. Three main sectors are defined according to the locations of the rural sites with respect to Paris: north-east (0-120°), south (120-240°) and north-west (240-360°). The distance between Paris center and rural stations is about 50 km. By determining the dominant sector for particles in the last four hours before reaching Paris, the upwind rural site can be deduced. Figure 2 gives an illustration for three particular days. Due to the complexity of wind fields, this procedure is certainly too simplistic to account for all meteorological situations that may occur over the Paris region (e.g. back trajectories originating from more than one sector, recirculation). However, all these problems relative to the choice of the appropriate upwind

rural site are tackled by the quantification of advected contributions uncertainties in which all the three rural concentration values are included, as described in the next section.

Following Lenschow et al. (2001), the methodology thus relies on the assumption that (i) both the PAR station and the upwind rural station are representative of urban background and advected regional background, respectively, and that (ii) no significant changes affect the aerosol chemical composition between rural sites and the edge of the agglomeration (e.g. photochemistry, thermodynamic equilibrium). Concerning this latter hypothesis, the short distance between rural sites and Paris is likely to prevent most SOA production during the transport of air masses, as well as too strong discrepancies in thermodynamic conditions. The validity of the first hypothesis is further discussed in Sect. 4.2. In addition, it should be noted that PM species concentrations are quite similar from one rural site to another, at least in average over the year. However, strong discrepancies sometimes appear for the OM species, larger values at the RNE site being probably related to some local wood burning (domestic heating) emissions at this site. The RNE rural site can thus not be considered as representative of the OM rural background, but this local wood burning pollution is not assumed to impact significantly the other species. In order to avoid invalidating all data from the RNE site, OM concentrations are invalidated only when the discrepancies with the two other sites are stronger than 30% (see analysis and a discussion of this threshold value in Supplement, Sect. S.3).

4.2 Uncertainty discussion

In this section, we first discuss the uncertainties associated to the choice of the up-wind rural station. Uncertainties related to the $PM_{2.5}$ urban background heterogeneity in the Greater Paris, and consequently the representativeness of PAR measurements, are then investigated. Note that, in all the paper, the term "urban" always refers to the urban background concentration in the city, thus including both advected and local contributions.

4.2.1 Uncertainties associated with the up-wind station choice

The methodology is based on the hypothesis that the chosen rural station is representative of the rural background air mass advected toward the city. We investigate here the uncertainty associated with the choice of the up-wind rural station.

For each day, up to three rural background stations may be available for estimating the advected contribution toward Paris. Considering the regular distribution of these stations in all directions around Paris, let us assume that the exact value of the advected contribution is bounded by the lowest and highest concentrations among them. For each day *i*, the

concentration range among rural stations can thus be seen as the possible absolute error e_i on advected contribution. Based on our first hypothesis, this value represents an upper limit of the uncertainty since the additional information given by the wind direction that allows the choice of a particular station is not taken into account. Considering a period of n days, from error propagation, the absolute uncertainty on the averaged advected contribution can then be estimated as:

$$\overline{e_n} = \frac{1}{n}\sqrt{\sum_{i=1}^{n} e_i^{\,2}} \qquad (1)$$

4.2.2 Urban background heterogeneity

The methodology used in this work is also based on the assumption that the PAR station is representative of the Greater Paris urban background. However, the $PM_{2.5}$ heterogeneity can be significant in this area. Although the model grid cell corresponding to the measurement site (with 3 km horizontal resolution) has been chosen for comparison purposes, the simulations may not correctly express the larger scale intra-urban variability, or the sub-grid variability. This would partly prevent us from interpreting the observed differences in the local contributions as representative for the whole urban area.

Three other TEOM-FDMS are available in the Greater Paris from the AIRPARIF network (in the suburban area of Paris), measuring both $PM_{2.5}$ semi-volatile and non-volatile parts. The top panel of Fig. 3 shows the $PM_{2.5}$ concentration range of this station set including the PAR station, the mean $PM_{2.5}$ concentration of these four stations, and the concentration measured at the PAR station. Discrepancies to the mean daily $PM_{2.5}$ concentration (bottom panel) range from -15.5 to +22.7 μg m^{-3}, but most of values (89% of available data) do not differ more than ±5 μg m^{-3} from the mean. Large discrepancies may be due to specific local events or stagnant conditions preventing air masses from horizontal mixing. This latter situation occurs for instance the 28 October during which the lowest wind speed of the whole period is measured at the MONTSOURIS meteorological station (48.822°N, 2.337°E) in the center of Paris (daily mean around 1 m s^{-1}). This day corresponds to the third largest $PM_{2.5}$ departure from the mean, which is also visible with PM_{10} or NO_2 (not shown). In average, the $PM_{2.5}$ concentration at the PAR site is slightly lower than the mean urban background concentration, with a discrepancy of -0.4 μg m^{-3}.

Similarly to advected contributions, we define the absolute uncertainty on the urban background concentration as the maximum concentration range between this panel of urban

stations. However, as only $PM_{2.5}$ data are available in the Paris region, the approach cannot be applied to main chemical constituents of $PM_{2.5}$.

4.2.3 Overall contribution uncertainties

All these uncertainties are given in the Table 3 for all compounds at three time scales (daily, monthly, annual), and reported in Fig. 9 for each month. As local contributions (L) are deduced from advected ones (A) and urban background concentrations (U) by simple subtraction (L=U-A), from errors propagation it follows that these uncertainties on imports (e_A) represent a minimum for the local contribution:

$$e_L = \sqrt{e_U{}^2 + e_A{}^2} \qquad (2)$$

to which have to be added the uncertainty associated with the urban background concentration (e_U). As seen before, this latter uncertainty e_U cannot be estimated for PM chemical constituents (as for $PM_{2.5}$ mass) due to missing additional observations. The uncertainty on their local contributions is thus not fully quantified (as for $PM_{2.5}$ mass), but has a low limit given by the uncertainty on their imports. This might lead to an underestimation of this uncertainty.

At the daily scale, these uncertainties are quite strong. In relative terms, they prove to be too strong to be compared to model results. Moreover, as most compounds are mainly advected (except EC), uncertainties on local contributions are much stronger than on advected ones (despite their partial quantification). This explains the significant noise in daily time series. They are seriously reduced for monthly contributions, which justifies our choice to discuss results at this time scale. Such a decrease comes from a simple mathematical consideration, that the uncertainty decreases with the root of the number of days, when considering errors on individual days as independent. Except for some chemical constituents during specific months of relatively low imports (EC and OM in October, nitrate in summertime), relative monthly uncertainties on advected contributions remain below ±20%. Concerning monthly local contributions, values remain reasonable for EC (mainly local), ranging between ±4 and ±11% depending on the month. Local OM monthly uncertainties are more critical (±43% in average), particularly during wintertime (January and February, with absolute uncertainties above 1 μg m^{-3} for local contributions below 0.8 μg m^{-3}) when they almost reach a factor of two. They are much stronger for secondary inorganic compounds (to a lesser extent for nitrates), due to very low monthly local contributions, often largely below the absolute uncertainty. However, several months show a non negligible local contribution such as: October, December and January.

Local $PM_{2.5}$ contribution uncertainties show an average value around ±41%, with strongest values exceeding ±40% in September, February and March (±51, ±47 and ±52% respectively). Uncertainties at the annual scale are below ±5% for advected contributions, and below ±20% for local contributions for most compounds (expect ammonium and sulfate that have almost negligible annual local production).

Based on these results, it follows that the choice of the up-wind rural station does not affect very much the discussion of monthly advected contributions, compared to measurement uncertainties. However, most of local contributions show larger uncertainties (particularly local OM) that, even if they are usually associated with very low contributions, have to be taken into account in the discussion of the comparison with simulation results.

4.3 Model evaluation

The idea of the approach developed in this paper consists in evaluating separately the local and advected contributions. After interpolation of concentrations at all four sites, simulated contributions are derived in the same way as observed ones. We will attempt to answer the following question: is the CHIMERE model (as implemented in the ESMERALDA platform) able to correctly simulate both advected and local contributions for the main chemical constituents of $PM_{2.5}$? Comparisons between measurements and simulations will be achieved on an annual and monthly basis.

Statistical metrics used in this paper are defined as following:

- Mean bias: $MB = \frac{1}{n}\sum_{i=1}^{n}(m_i - o_i)$ (3)
- Normalized mean bias: $NMB = \frac{\frac{1}{n}\sum_{i=1}^{n}(m_i - o_i)}{\bar{o}}$ (4)
- Root mean square error: $RMSE = \sqrt{\frac{1}{n}\sum_{i=1}^{n}(m_i - o_i)^2}$ (5)
- Normalized root mean square error: $NRMSE = \frac{\sqrt{\frac{1}{n}\sum_{i=1}^{n}(m_i - o_i)^2}}{\bar{o}}$ (6)

- Correlation coefficient: $$R = \frac{\sum_{i=1}^{n}(m_i - \overline{m})(o_i - \overline{o})}{\sqrt{\sum_{i=1}^{n}(m_i - \overline{m})^2 \sum_{i=1}^{n}(o_i - \overline{o})^2}} \quad (7)$$

Where m_i and o_i are the modelled and observed concentrations at time i, respectively, and $\overline{m}$ and $\overline{o}$ their average over the period.

5 Results

This section presents the model evaluation results. In a first part, the meteorological simulation is evaluated in the center of Paris (Sect. 5.1). A quick overview of observed pollution regimes during the whole year is presented in a second part, with annual average results from observations (Sect. 5.2). Simulation annual results are then described (Sect. 5.3), followed by a description of results for each individual main chemical constituents of $PM_{2.5}$ focussing on seasonal variations (Sect. 5.4 to 5.7). Implications for model evaluation are finally discussed (Sect. 5.8).

5.1 Meteorology evaluation

Current meteorological parameters — temperature, wind speed and direction, relative humidity (RH) and precipitation — are measured in the center of Paris at the MONTSOURIS station. Figure 4 shows the comparison with MM5 simulations used in the CHIMERE CTM, statistical results are given in Table 4.

The model simulates well temperature and RH, with only a slight bias of -1°C and +3.1%, respectively, while NRMSE remains low (around 13% for RH). According to diurnal profiles (not shown), these biases occur mainly during the night and in the morning. Wind speed also shows a very low bias (+0.1 m s^{-1} or +2% in relative), but with a stronger NRMSE around 30%. Again, discrepancies are stronger during the night, the early morning and the early evening. With mean discrepancies around 11.8°, simulation of wind direction appears to be satisfactory as well. Considering the difficulty to correctly simulate precipitations, the bias in simulations (-0.02 mm or -34% in relative) is quite good. The model is nevertheless not able to correctly catch all the events or sometimes wrongly predicts events, leading to an important NRMSE (around 850%, reduced to 205% with daily values). However, such a large error is expected since rain episodes can be very local, making difficult to properly locate them in the meteorological models.

Boundary-layer height (BLH) estimations are available during the PARTICULES campaign from an aerosol lidar at the SIRTA platform (48.712°N, 2.208°E), located in the Paris suburban background at about 20 km in south-west of the city center (Haeffelin et al., 2011). Figure 5 shows modelled and observed diurnal profiles.

On a yearly average over the whole year, the model overestimates the BLH at each hour of the day except between 16:00-19:00 UTC, and more particularly during night-time (by about a factor of two). However, these averaged results hide very different monthly tendencies, with the strongest overestimations in November, December, February and March, and better results in September and October. However, such comparisons remain quite tricky since strong uncertainties still affect observed BLH estimations, particularly during transition to nocturnal stable BL in the afternoon (because of the development of a residual BL) and during nighttime or in the presence of clouds (Pal et al., 2013; Cimini et al., 2013). Additionally, algorithms do not work in case of rain.

It has also to be noted that urban heat island (UHI) effects are not taken into account in input meteorological data, which can lead to an underestimation of the simulated BLH in the city center (mostly in winter), due to unaccounted anthropogenic urban heat fluxes. For the Paris megacity, urban-rural temperature contrasts up to 7°C have been noticed at night (Lac et al., 2013). Since SIRTA is a suburban site, the BLH overestimation may be compensated in Paris by this UHI effect not accounted in the model. In the framework of the CO2-MEGAPARIS campaign in March 2011, the UHI effect in the Paris agglomeration (with eight deployed lidars) has been investigated, leading to nocturnal BL differences between urban and adjacent suburban areas of +63 m (+45%) on average (Pal et al., 2012). These authors also measured a slower urban BLH decay during the late afternoon/evening transition (500 m h^{-1} against 600 m h^{-1} in suburban areas). These results may thus indicate a reduced model error in the Paris center (since BLH average simulations in the city center and at SIRTA only slightly differ). Note that, to balance that missing UHI effect, a minimum BL height is fixed in the model over urban areas. In our case, the value of 150 m is chosen for a 100% urban cell (and decreases proportionally to the amount of non-urban landuse within the cell), based on the 2nd percentile (120 m) of BLH measured at the SIRTA suburban site.

5.2 Annual average speciation budget overview

In this section, the focus is put on observation results, while model results will be investigated in the next sections.

The annual mean $PM_{2.5}$ concentration at the PAR site measured with the gravimetric method is 15.1 μg m^{-3}, with daily values ranging from 4 to 63 μg m^{-3} over the year (Fig. 6). The variability (standard deviation of 8.6 μg m^{-3}) strongly depends on the wind regime, with large episodes mostly linked to advection of continental air masses from the north-east wind sector as indicated by back trajectories over a few days. This leads to much stronger mean $PM_{2.5}$ concentrations during this regime than during the two other ones (average concentration of 20.9 μg m^{-3}, against 14.4 and 11.7 μg m^{-3} for south and north-west sectors, respectively). Back-trajectory results give an occurrence frequency of 30%, 26% and 44% for NE, S and NW sectors, respectively (4 hours before Paris).

Most $PM_{2.5}$ advection episodes occur during winter and spring, few others at the end of September and October. Independently to the wind regime, $PM_{2.5}$ appears to be mostly advected over Paris. Table 5 clearly shows that strongest aerosol loads are brought by north-east winds, with much larger variations compared to the two other sectors.

The mean chemical composition of observed urban background $PM_{2.5}$ is composed by 11% of EC, 43% of OM, 14% of nitrate, 13% of sulfate and 8% of ammonium. Figures 7 and 8 present the local and advected contributions for $PM_{2.5}$ and its main chemical constituents. Model results are also reported on these figures but will be discussed in the next section. Relative contribution values are reported in the Table 6. It confirms the importance of imports in the $PM_{2.5}$ urban background (71%). Estimated daily local contributions remain below 20 μg m^{-3} during the whole period and show a large day-to-day variability, partly due to the previously mentioned uncertainties in the estimation method.

Observed imports are mainly composed of OM and secondary inorganic species (respectively 41% and 42% of total advected $PM_{2.5}$, respectively), while production within the Paris region mainly consists of carbonaceous compounds: OM contributes to 45% of the total local $PM_{2.5}$ and EC to 29%. This local contribution represents 74 and 31% of the urban EC and OM, respectively. Secondary inorganics species are essentially advected from outside.

Negative values can be observed for local contributions. They are related either to noise in the analysis procedure (see Sect. 4.2), but can also reflect losses on the way from the rural to the urban site, due to dry and wet deposition, chemical lost and/or thermodynamical equilibrium changes for secondary inorganic and organic aerosol.

5.3 CHIMERE average budget results

Statistical results over the whole period are given in Table 7. On average, the CHIMERE model rather well retrieves the urban background $PM_{2.5}$ concentrations, with a slight positive bias around +16%, i.e. in the range of uncertainty of filter measurements. With a correlation (R) of 0.59 and a NRMSE around 56%, the $PM_{2.5}$ scores are in the upper range of CTM performances computed by Stern et al. (2008) for several models, over a European domain and a 80-day period. For the main chemical PM constituents, the poorest results concern EC which is significantly overestimated (NMB of +70% and NRMSE 104%). Nitrate and ammonium are overestimated in the model (+23% and +10% respectively) which may be partly explained by negative sampling artefacts as discussed previously. Conversely, OM underestimation (-21%) may be even stronger due to possible negative artefacts. Carbonaceous compounds and sulfate show the lowest correlation (R below 0.54), while ammonium nitrate variability is correctly captured by the model with correlations above 0.7. Note that an overestimation of simulated dusts in the fine mode also affects the results on $PM_{2.5}$.

However, these urban background results hide a more complex picture in terms of imported versus local contributions. Indeed, results on imported $PM_{2.5}$ contributions show a reasonable agreement with observations (NMB of +1.1%), but with large error compensations between ammonium nitrate and the other compounds. The nitrate overestimation (+63%) is too strong to be fully explained by the filter measurement uncertainty. Despite its large RMSE (more than a factor of two), this compound has the best correlation (0.73), and may significantly contribute to the good correlation obtained for the imported $PM_{2.5}$ (0.58). The lowest correlation concerns OM (0.33) that goes also with a strong negative bias (-59%). Negative biases are rather small for sulfates and EC (below -18%), but errors and correlations remain poor (NRMSE above 57% and R below 0.48).

The CHIMERE ability to simulate local contributions appears even more critical. Local $PM_{2.5}$ appears overestimated (+51%), with errors stronger than a factor of two (117%) as well as low correlation (0.41). Statistical results are bad for most individual compounds, carbonaceous species being overestimated by about a factor of two (+103 and +76% for EC and OM, respectively), and inorganic species underestimated also by a factor of two (except for sulfate which local contribution remains close to zero). Errors typically range between a factor two to four, while correlations are rather low, 0.45 for EC, 0.23 for OM and around 0.1-0.3 for inorganic compounds. Spatial and temporal heterogeneities in emissions and in dispersion conditions not expressed in the model in spite of its 3 km horizontal resolution probably

explain a part of these large RMSE values on locally emitted compounds (e.g. carbonaceous compounds).

Modeled and observed imported and local contributions for $PM_{2.5}$ and its main chemical components are represented in Fig. 9. Monthly contribution observations uncertainties quantified in Sect. 4.2 are also reported. The following sections investigate in more detail these model results for each individual compound.

5.4 Elemental carbon local and imported contributions

Urban background observations show that elemental carbon in the Greater Paris region is mainly due to local emissions, with an advected contribution of around 1/3 of the yearly mean concentration. Simulated and observed imported EC levels show a clear seasonal variation with higher concentrations in wintertime and in the early fall period (September and October). The CHIMERE model retrieves quite well the imported EC during most of the year, with a negative bias of -18% (except during the early fall period where bias is significantly higher). This bias falls in the range of measurement uncertainty of 20 %, and the ±25% maximum monthly uncertainty in determining background condition (see Sect. 4.2). In addition, regional EC emissions still have large uncertainties. Even at the global scale, considering uncertainties in emission factors, types of emissions, fuel use, EC emissions uncertainties have been estimated around a factor of two by Bond et al. (2013). Also model transport and sink processes by deposition are uncertain (Solazzo et al., 2012; Vautard et al., 2012). Given all these error sources, the agreement can be regarded as satisfactory.

Conversely, local EC contributions are significantly overestimated by the model, with a relative mean bias around a factor of two. The observed month-to-month variability is quite low (monthly averages around 1 $\mu g\ m^{-3}$), in contrast with a larger simulated variability with monthly peak values in September, October and January. Surprisingly, while imported EC shows a seasonal variation with stronger values during cold months, we do not observe similar variability for the local (Paris region) contribution of EC, although higher local emissions associated with domestic wood burning and lower mixing heights are expected in winter. This may indicate a predominance of traffic related EC at the local scale, compared to woodburning EC for which contribution is expected to increase further away from the Paris center. According to the ESMERALDA inventory used, road and non-road transport represent 63 and 13% of the EC emissions in the Greater Paris agglomeration, respectively, while 20% comes from residential heating. This is confirmed by an independent study during the MEGAPOLI

winter campaign in which 88% and 12% of EC particle mass was apportioned to fossil fuel and biomass burning, respectively, using the ATOFMS data, compared with 85% and 15% respectively for BC estimated from the aethalometer model (Healy et al., 2012).

EC biases in CHIMERE appear highly variable from one month to the other, the strongest ones occurring in September, October and January. Emission related errors are not expected to show a similar month-to-month variability. Alternatively, pollutant dispersion, through vertical and horizontal mixing and advection, may significantly contribute to the simulated month-to-month EC bias. The combination of very weak wind speed (lower than 1.5 m s^{-1}), low BLH (up to 150 m, i.e. the user-fixed minimum value in urban areas) and fresh emissions (mostly related to traffic) during several hours may result in very high simulated peaks on particular days. Such peaks are mainly simulated for particular days during the months of September, October and January for which monthly means are affected, while observations do not show such events. These specific days are characterized by episodes usually lasting few hours during morning and evening, with hourly EC concentrations reaching values higher than 10 µg m^{-3} (up to 20 µg m^{-3} the 26 October). A small shift of the time at which convective BL starts to grow can lead to very large discrepancies. Similarly, as previously mentioned, the transition from convective to stable BL in the evening remains difficult to define properly, and is thus associated with significant uncertainties. Also vertical mixing within the boundary layer remains a potential error source that is difficult to quantify in the absence of vertical profile measurements. Local EC simulations with the lowest overestimations appear during months with the highest BLH overestimation (November, December, and February). This suggests a potential overestimation of EC emissions in the local inventory. In addition, the monthly error variability may also be explained by wind speed errors. For instance, November simulation shows the best results, but also the strongest overestimation of wind speed (bias of +0.91 m s^{-1}, +23% in relative). It is worthwhile noting that an increased uncertainty on locally emitted compounds such as EC (and OC) may arise from the high resolution of CHIMERE simulation and input data (e.g. emissions, meteorology), as it was shown for ozone (Valari and Menut, 2008).

In order to minimize errors induced by pollutant dispersion, the local EC contribution can be normalized by the NO_x ($NO+NO_2$) concentration measured in the Paris center (PA12 station from the Airparif network (48.838°N, 2.394°E), nearby to the PAR station), as shown in Fig. 10. In this approach, NO_x emissions are assumed to be less uncertain than EC ones. Contrary to observations that follow a clear seasonal variation with a winter minimum, simulated EC/NO_x ratios show a very small month-to-month variability, staying in the range 0.024-0.033 µg m^{-}

^{3}.ppb^{-1}, in good accordance with the ratio in the emission inventory of 0.038 given for both the residential and road transport sectors. CHIMERE overestimates this ratio, particularly during winter, when observed ratios decrease.

Consequently, the Greater Paris EC emissions in CHIMERE may be overestimated, at least during winter time, by up to a factor of two, while a satisfactory EC/NO_x ratio is found in summer.

Such positive biases of EC in Paris have already been reported with the CHIMERE model using a quite similar (at least for Paris region) $PM_{2.5}$ inventory during spring 2007 (Sciare et al., 2010) and summer 2009 (Zhang et al., 2013). However, during that latter period, with similar Paris $PM_{2.5}$ emissions (and quite similar EC speciation for the road transport sector) and another chemistry-transport model, as well as different meteorological data (taken from WRF rather than MM5 model), Couvidat et al. (2013) have found a slightly negative bias in Paris, but a positive one at a suburban site. However, all these studies have considered urban background concentrations, rather than a local increment, and are thus not directly comparable to our work because of (i) significant advected EC contribution (~1/3) and (ii) potential error compensation between imports and local production.

5.5 Organic matter local and imported contributions

On average during the whole year, OM observations show that it is the dominant compound of $PM_{2.5}$, with a contribution of 42% to urban background $PM_{2.5}$ levels. Observations also show that it is mainly advected (69%), with a strong seasonal variation with maximum imports occuring during winter. Periods with the largest contributions of imported OM are observed from December to February with daily advected contributions reaching up to 20 μg m^{-3}.

The CHIMERE model clearly fails to simulate such high imported OM levels, with, for instance, more than a factor of five of underestimation for the month of January which cannot be explained by the 14% uncertainty in determining imported contribution (see Sect. 4.2) and by the measurement uncertainties. If observed OM values were underestimated, as suggested in Sect. 2, these underestimations would be even larger. In opposition to observations, imported OM simulated by CHIMERE during winter are even lower than during summertime. Due to low photochemical activity in winter, the contribution of imported SOA (relatively to OM) in the model remains small, with values around 20-30% and showing a predominant (70-90%) biogenic origin (BSOA). CHIMERE provides much better results during summer, with much higher simulated SOA imports, accounting for 40 to 80% of OM. Again, this SOA is mostly

biogenic (more than 90%), with significant contribution of isoprene oxidation that provides 40% of the total SOA. During the whole year, the daily anthropogenic SOA (ASOA) simulated concentration remains below 1 μg m^{-3} while BSOA reaches levels above 6 μg m^{-3}.

Underestimated European POA emissions may partly explain the wintertime negative biases in imported OM levels. Indeed, POA emissions still have large uncertainties, because of the various potential sources, e.g. traffic, residential heating (Sciare et al., 2011), or unaccounted cooking (see for instance Crippa et al., 2012) and the difficulty to properly determine emission factors (Bond et al., 2013). As one of the major sources in winter, uncertainties in wood burning emissions are probably responsible to a large extent of this underestimation. This is especially due to the large range of emission factor values depending on the equipment (open fireplace, closed inserts, boilers, stoves) (Nussbaumer et al., 2008), the lack of local data in bottom-up approaches (e.g. consumptions, equipment type) and conversely, the difficulty to find appropriate spatial distribution proxies in top-down approaches (stronger rural than urban per capita emissions). Another factor of uncertainty is the semi-volatile nature of POA emissions (Robinson et al., 2007) ignored in our simulations. Additionally, as the fraction of volatilized POA depends on the ambient OA concentration, no consensus yet exists on the dilution conditions at which POA emission factor (EF) measurements are conducted in lab experiments. While Zhang et al. (2013) consider that these measurements are done at low dilution and thus do not apply any correction to POA emissions, Couvidat et al. (2012) argue that dilution is much stronger and finally use a factor of five of correction. At this stage, no elements allow us to conclude on this point, especially as inventories usually aggregate EF from various databases in which experimental conditions are probably different.

Levoglucosan measurements are available during the whole year at the PAR and RUS stations and can be used to quantify the spatial distribution of domestic wood burning in the region of Paris. If we assume that measurements at this rural station are representative of the regional background advected toward Paris, it is thus possible to derive local and advected contributions using the Lenschow approach (Fig. 11). In this figure, levoglucosan appears to be mostly advected, which suggests a significant contribution of wood burning OM imports. A local production in the Paris region also clearly appears (around 30% in December).

Wood burning has shown to significantly contribute to urban background $PM_{2.5}$ levels during winter 2005 in Paris, around 20±10% (Favez et al., 2009). Sciare et al. (2011) have estimated this wood burning contribution to represent 15±11% of $PM_{2.5}$ during winter 2009 at a suburban site of Paris. Positive matrix factorization (PMF) of aerosol mass spectrometer (AMS)

measurements gives a SOA contribution of more than 50% of OM in Paris, including also a part of aged woodburning OM (Crippa et al., 2012). As advected OM is mainly composed of POA in the simulation, its underestimation is probably partly related to missing SOA formation pathways in the model. The volatility-basis set (VBS) approach (Donahue et al., 2006) takes into account the POA volatility and reactivity, as well as the chemical aging of SOA (Robinson et al., 2007). In EMEP model simulations over six years, Bergström et al. (2012) have shown that the VBS approach can increase the OA background over France, Benelux, Germany and Eastern Europe from 2-3 to 3-5 μg m^{-3}. During wintertime with smaller oxidant levels, non-oxidative SOA formation pathways occurring in the aqueous or aerosol phase and leading to high molecular-weight products are thought to be important (Kalberer et al., 2004, Carlton et al., 2008, Hallquist et al., 2009; Ervens et al., 2011).

Conversely, simulated local OM appears overestimated, more than the uncertainty of observed contribution (±69% in average). Note that the unexpected local OM seasonal variation, with the lowest contributions in January and February, and the strongest in October, is still within the range of uncertainty on monthly values for local contributions (up to ±93%, Fig. 9). Model biases show a large month-to-month variability during the year, which may be partly due to this uncertainty. In addition, since simulated OM remains predominantly composed of locally emitted POA, a chemically inert species in CHIMERE, the high variability in monthly biases is partly explained by dynamical errors (BLH, wind speed), as indicated by the strong correlation (R=0.97) between OM and EC monthly local contributions.

By considering the ratio of OM versus EC local contribution, it is possible to investigate in more detail this latter point. Figure 12 shows the evolution of this ratio over the year. Observations show a local average OM/EC ratio around 1.7 with a significant monthly variability, but no clear seasonal variation. Given the measurement uncertainties (around 20% for EC and up to 60% for OM), this is still consistent with the average value of 1.3 found in CHIMERE simulations (NMB of -19%). Assuming that a major part of local OM is of primary origin, the local OM overestimation is thus related to a similar EC overestimation. This indicates that emission errors are probably more related to the total emission amount than to the $PM_{2.5}$ speciation. The simulated local OM/EC ratio of 1.3, closer to the OM/EC emission ratio of 0.96 for road transport in the Greater Paris region, than to the ratio of 5.76 for residential heating, also reflects a dominant road transport contribution in the city center. It can be noted that the OM/EC emission ratio of 0.96 for road transport is rather consistent with a value of

0.78 derived from OM and EC measurements during the PARTICULES campaign at a traffic site (located at the Paris urban highway). Differences could be due either to the specific OM/EC emission factors for diesel and gasoline vehicles, around 0.5 and 2.8 respectively, the representativity of the composition of the vehicle fleet at a given site for urban background, or again to measurement uncertainties.

As previously mentioned, another factor of local OM overestimation may be the missing evaporation of semivolatile POA emissions. By considering the Paris ambient conditions (in terms of temperature and OM concentrations), one can derive that as much as 40-80% of POA emissions could be volatilized (see analysis and Fig. S4 in the Supplement). This is expected to partly explain the CHIMERE overestimation of the OM local contribution. However, it is to be noted that, according to this approach, these lower emissions are balanced by the POA reactivity that increases the amount of SOA (i.e. oxidized POA, OPOA), but with a certain delay in time and thus mostly outside of the agglomeration (Zhang et al., 2013). It is also important to remind that large uncertainties exist on the amount of semivolatile organic material taken into account in POA emission factors.

As a conclusion, the underestimated OM advection during wintertime is probably both due to lacking woodburning emissions and missing SOA formation pathways in the model. Additional SOA formation pathways would also increase SOA advection in summer, as shown by CHIMERE simulations of the MEGAPOLI summer campaign including the VBS scheme (Zhang et al., 2013). Given the possible underestimation in OA due to evaporation (see Sect. S.1 in Supplement), this would not be inconsistent with measurements. Concerning OM local contributions, apart from their uncertainties, errors in PM emissions, combined with the unaccounted POA volatility, and errors in dynamics probably explain a large part of their overestimation as well as the CHIMERE's difficulty to catch their variability.

5.6 Nitrate contributions

Nitrate is the second largest contributor to urban $PM_{2.5}$ in this study. The largest episodes occur in March and April, mostly due to nitrate advection from outside (Fig. 9). This leads to a seasonal variation of imported nitrate with higher concentrations reached during springtime (higher NH_3 emissions due to fertilizer use). Despite the low photochemistry, some strong nitrate episodes are observed in winter. Nitrate formation during these seasons is due to the low volatility of ammonium nitrate at cold temperatures.

The CHIMERE model simulates rather well the seasonal variation of the advected contribution (R of 0.73), but with a significant positive bias (+1.4 μg m^{-3}, +63% in relative), much larger than uncertainties on advected contribution (below 20% from October to July). The largest overestimations occur in autumn and spring (with more than a factor of two). As explained in Sect. 2, positive biases may be partly due to errors in measurements, related to volatilisation artefacts during sampling. They probably explain a large part of the overestimation, mainly in autumn and spring when temperature and potential filter artefacts increase but temperature remains low enough to allow the existence of particulate-phase ammonium nitrate.

Errors in the simulated meteorology, temperature and RH, modifying the thermodynamical equilibra may also partly explain these results (see analysis in Sect. S.5 in the Supplement). Such errors become more problematic at mild to hot periods (June for instance) since, through its dissociation constant, the temperature dependance of the ammonium nitrate thermodynamic equilibra increases with temperature (Seinfield and Pandis, 2006). Clear temperature underestimation are sometimes observed over all Europe (e.g. in June, see Fig. S7 in the Supplement). This may increase the amount of nitrate in the particulate phase and consequently decrease the dry deposition of HNO_3 (significantly stronger compared to nitrate, Baumgardner et al., 2002). This may finally induce an overestimation of total nitrate (HNO_3 + particulate NO_3^-) reservoir over Europe, which can eventually lead to overestimated nitrate imports, depending on the thermodynamical conditions.

The nitrate overestimation may also be related to uncertainties in the simulated precursor gas concentrations (NH_3, HNO_3). The G_{ratio} metric provides information on which species is the limiting factor in the ammonium nitrate formation (Ansari and Pandis, 1998; Pinder et al., 2008). It is defined as (all concentrations being expressed in mol m^{-3}):

$$G_{ratio} = \frac{[NH_3] + [NH_4^+] - 2[SO_4^{2-}]}{[HNO_3] + [NO_3^-]} \quad (8)$$

Values above 1 indicate a HNO_3-limited regime, while values below 1 indicate a NH_3-limited regime. In this expression, the numerator, also known as the free ammonia indicator ($F\text{-}NH_x$), represents the available ammonia after neutralization of sulfates, one mole of sulfate removing two moles of ammonia. The simulated G_{ratio} indicates a dominant HNO_3-limited regime over the continent, while the regime is NH_3-limited over the sea. This result is in accordance with several previous studies performed over Europe (Pay et al., 2012; and references therein). Accordingly, if nitrate overestimation is related to overestimated emissions, this mostly

concerns NO_x emissions and chemistry rather than NH_3. However, this would not be consistent with Konovalov et al. (2006) who have shown, through an inverse modelling exercise over Europe with satellite measurements, that NO_x emissions from the EMEP inventory (used in our study, outside the refined domain) have a tendency for an underestimation of several tenths % in the Benelux and Rhine Ruhr region, which are important NO_x sources contributing to nitrate advection to Paris. The nitrate overestimation may also be explained by a too high conversion of NO_x into HNO_3. Such positive biases on nitrates are not in accordance with some recent papers (Pay et al., 2012) that simulate significant negative biases over Europe during a whole year (MB of -1 μg m^{-3}, NMB of -50%).

Concerning local contributions, observations give positive or near zero contributions, with a rather strong month-to-month variability, while the model does not simulate any particular nitrate production in the Paris region. Uncertainties in local contributions are large (Fig. 7), but for several months as October, December and January, local nitrate production is significant, reaching for instance 2.0±0.4 μg m^{-3} in January. According to the model, nitrate production is significantly underestimated. Actually, the Greater Paris region appears to be a nitrate sink, particularly during later spring and early summer. However, these negative local contributions usually remain low. As the G_{ratio} is mostly above unity in Paris (3.2 in average), HNO_3 is usually the limiting species. During winter, uncertainty in the speed of heterogeneous NO_x to HNO_3 conversion, one of the major pathways in simulations, is large (e.g. Jacob et al., 2000) and may explain these discrepancies. It is both related to uncertainty in the conversion mechanism (e.g. accommodation coefficients) and in input data (aerosol surface, relative humidity). On an hourly basis all along the period, a NH_3-limited regime is also sometimes simulated (during about 13% of the period), which may be a factor of nitrate underestimation in case of missing NH_3 emission sources, like the traffic source in our case.

5.7 Sulfate contributions

Observed monthly sulfate imports range from 0.8 to 3.2 μg m^{-3}, with the highest values reached in September 2009, spring and winter. Imports are lower in autumn and early winter probably due to the recurrent south-westerly wind regime (particularly in November) associated with low SO_2 emissions in this direction. These low emissions do not appear to be compensated by the higher RH (around 83% in average in November) brought by oceanic air masses that allows fast aqueous phase sulfate formation (Kai et al., 2007; Rengarajan et al., 2011). In winter, the

strong monthly contributions are driven by some very high imports of different durations from north-east (Fig. 9), while regional background concentrations remain low. Since photochemistry is expected to be limited during the winter season, these strong imports during the cold season may be mostly related to aqueous phase sulfate formation from the large SO_2 emissions in Benelux and Western Germany. The situation is quite different in spring, with lower sulfate peak values during episodes but higher background the rest of the time. This leads to higher monthly values, despite lower SO_2 emissions.

On average, the CHIMERE model simulates rather well the advected sulfate, with a mean bias of about -17%. Larger negative biases are found in June, September and winter months, and cannot be explained by uncertainties in the observed advected contributions (below 14%). The underestimations in January, February, June and September are mainly due to missing or underestimated advection events. Apart from uncertainties in their temporal behaviour, SO_2 emissions are expected to be reasonably quantified, and the sulfate underestimation may thus be partly explained by errors on transport and/or gas and aqueous phase sulfate formation. Aqueous phase formation, the major formation pathway at least during winter, depends on several parameters not well constrained in our simulations such as the cloud water content and the pH.

Observations show quite low sulfate local production in the Greater Paris, except in January where the monthly production is quite stronger and appears significant (0.7 ± 0.1 µg m^{-3}). During this month, the observed production essentially occurs on January 18 during a fog event associated with low wind speed (around 1 m s^{-1}). Such conditions enhance fast heterogeneous sulfate formation, leading to a daily local contribution above 4 µg m^{-3}. This event has been more precisely described by measurements during the concomitant MEGAPOLI winter campaign (Healy et al., 2012). As a slow process (except during fog events), sulfate formation thus remains low at the local scale in Paris, and is more likely to occur in the plume of the city. Concerning this particular fog event, the CHIMERE model manages to capture this sulfate production peak, but not to its full extent (negative bias around -70%). Uncertainties in observed local contributions are stronger during the other months, explaining the quite noisy monthly signal and preventing us to conclude on a noticeable sulfate production. Besides the January fog event, the model also simulates very low sulfate production in the Greater Paris, and thus stays reasonably close to observations.

5.8 Implications for model evaluation

As various error compensations in $PM_{2.5}$ simulation have been underlined in the previous sections, it appears interesting at this stage to evaluate the CHIMERE model performance not only in terms of urban background concentrations, but also considering both advected and local contributions.

Boylan and Russel (2006) have proposed to evaluate CTMs performance with the Mean Fractional Bias (MFB) and the Mean Fractional Error (MFE), two statistical metrics integrating the fact that both simulations and observations are subject to uncertainties, which appears particularly suited for aerosol in our case. Both statistics are defined as follows:

$$MFB = \frac{1}{n}\sum_{i=1}^{n}\frac{(m_i - o_i)}{(m_i + o_i)*0.5} \quad (9)$$

$$MFE = \frac{1}{n}\sum_{i=1}^{n}\frac{|m_i - o_i|}{(m_i + o_i)*0.5} \quad (10)$$

Where m_i and o_i are the modelled and observed concentrations respectively at time i.

By construction, MFB values are restricted to the ± 200% range, while MFE values can spread out from 0 to 200%. Another interesting feature is that they normalize large and small concentrations, which thus avoids giving too much weight to a particular season (e.g. wintertime nitrates). Boylan and Russel (2006) have also proposed some performance criteria and goals for PM depending on the average of the mean observed and mean simulated concentration so that to take into account the minor importance of errors in less abundant compounds (defined by an average concentration below 2.25 μg m^{-3}, corresponding to 15% of the US EPA annual air quality standard for $PM_{2.5}$, 15 μg m^{-3}):

- MFB goal : $MFB \leq \pm\left[170e^{-(\bar{o}+\bar{m})*0.5/0.5} + 30\right]$ (11)
- MFE goal : $MFE \leq 150e^{-(\bar{o}+\bar{m})*0.5/0.75} + 50$ (12)
- MFB criteria : $MFB \leq \pm\left[140e^{-(\bar{o}+\bar{m})*0.5/0.5} + 60\right]$ (13)

- MFE criteria : $MFE \leq 125e^{-(\bar{o}+\bar{m})*0.5/0.75} + 75$ (14)

These performance goal and criteria are widely used for CTM evaluation (Milford et al., 2013; Pay et al., 2012).

Simulation results for urban concentrations and both advected and local contributions are compared to these criteria in Fig. 13. Urban background concentrations (in black) meet both MFB and MFE goals for all $PM_{2.5}$ compounds, some of them being considered as minor ones. The OM urban concentration MFB and MFE (around -20 and 37% respectively) are in the upper range of CTM performances recently published (Bergström et al., 2012 and reference therein; Lane et al., 2008; Hu et al, 2009; Murphy and Pandis, 2009).

However, the previously described error compensations between advected and local contributions, as well as between compounds appear clearly. Concerning the advected part (in green), the nitrate overestimation is compensated by the OM underestimation, leading to very low bias on total $PM_{2.5}$ (MFB of +12%). MFE on these two compounds appears as more critical, satisfying only the performance criteria, but without damaging the $PM_{2.5}$ performance that stays below the 50% threshold (meaning that both biases tend to occur and partly cancel each other out simultaneously).

Concerning local contributions, MFB and MFE metrics do not accept negative values. We thus only consider local $PM_{2.5}$, EC and OM, and ignore secondary inorganic compounds (mostly negative). The local $PM_{2.5}$ contribution only reaches the performance criteria, but not the performance goal (MFB and MFE around +40 and 76% respectively). This is obviously due to the overestimation of EC and OM compounds that only meet the performance criteria thanks to their minor contribution (the performance goal being reached only on the MFE). MFB and MFE results are rather similar for both carbonaceous compounds.

Therefore, the overall CHIMERE model ability to reproduce urban background $PM_{2.5}$ speciation appears as rather satisfactory, but the simulation of advected OM and nitrate as well as local carbonaceous compounds still requires improvements to fulfill these performance goals.

6 Conclusions

An original approach to evaluate chemistry-transport models in terms of advected and local contributions rather than concentrations is described. Based on observations at both urban and

rural background stations, the estimation of advected contributions consists in the choice of the appropriate rural site considering back-trajectories data to localize the air masses origin, while local production is then simply deduced from the urban concentration by subtraction.

The methodology is applied to the CHIMERE model in the Paris region with a one-year daily measurements database of $PM_{2.5}$ and its speciation, in the framework of the PARTICULES project. On an annual basis, about 71% of the Paris urban background fine PM is related to imports from outside, mainly from the north-east. These air masses advect 87% of the inorganic secondary compounds, 69% of the OM and 26% of the EC. Artefacts in filter measurements (volatisation losses of semi-volatile material and adsorption gains of some gaseous species) introduce uncertainties, particularly for ammonium nitrate and organic matter. The net effect is mostly an underestimation of the measured semi-volatile material concentrations, estimated to around -30% in winter and up to -50% in summer.

Based on the concentration range between the three rural stations, uncertainties on both local and advected contributions associated with the choice of the up-wind rural station are also quantified. The representativeness of the urban background site is assessed for $PM_{2.5}$ by considering additional measurements at three other suburban stations of the AIRPARIF network in the Greater Paris. It appears that strong uncertainties affect daily local contributions of most compounds, leading to a significant noise in the signal. However, except for local contributions of inorganic species and OM during some months, uncertainties in monthly and annual contributions are significantly reduced and usually remain below measurement uncertainties.

The CHIMERE model simulates urban background $PM_{2.5}$ concentrations with only little bias (+16%). This is however due to error compensations between (i) advected and local contributions, (ii) different $PM_{2.5}$ compounds and (iii) periods of the year. Imports appear to be strongly underestimated in winter, particularly for OM and to a lesser extent sulfates, and slightly overestimated during the rest of the year mainly due to ammonium nitrate. Conversely, the local $PM_{2.5}$ production is significantly overestimated, essentially due to OM and EC.

Among the possible reasons for model errors, overestimated particulate matter emissions in the Paris region associated with dynamical errors (mainly boundary layer height) are pointed out to explain overestimations in these local contributions. A better simulation result of the local OM/EC ratio tends to demonstrate that errors are mostly related to the total PM emission amount rather than the PM speciation. Underestimated continental scale woodburning emissions and missing SOA formation pathways are probably responsible for the wintertime

underestimation in advected OM. A large part of the nitrate overestimation stays in the range of the filter measurement uncertainties. Influence of temperature and relative humidity errors on thermodynamical equilibria is investigated in Paris, and shows a limited impact on particulate nitrate simulation most of time (positive bias of +10% in average), except during mild to hot periods where errors can reach a factor of two on some episodes. Local and advected sulfate contributions are on the average well simulated, but individual long range transport episodes are missed or underestimated by the model.

Finally, the CHIMERE model appears reasonably suited for $PM_{2.5}$ air quality (AQ) forecasting, with urban concentrations fulfilling performance goals in terms of fractional biases and errors. However, efforts are still needed to reduce errors compensations between compounds. The diagnostic evaluation conducted here gives better insights on error origins (e.g. local emission inventories, meteorology), on which further improvements are required for a more detailed investigation of specific sources (e.g. wood burning OM).

The underestimation of OM wintertime imports appears as the most critical aspect, and efforts are needed to investigate if an underestimation of regional woodburning OM emissions (through emission factors and/or the dependance on temperature) can provide the missing material and/or if the too simplistic SOA formation scheme is likely to be responsible. Additional efforts are needed to evaluate emissions of carbonaceous material at the local scale, and as well as the local dynamic in urban environment (in particular the boundary layer height). A study of the chemical regime in Paris, in order to investigate which one, among nitric acid and ammonium, is the limited species in nitrate formation is also likely to better target the error source of the underestimated local nitrate production.

Such a large advected contribution in urban background $PM_{2.5}$ has important implications on environmental management. It notably shows that pollution reduction measures at the Paris scale alone are inadequate to prevent most exceedances of PM standards, thus underlying the necessity of integrated AQ management at the regional/continental scale. Similar studies should also be undertaken in other megacities in order to highlight the Paris agglomeration special feature (e.g. geographic situation, local orography). This study has focused on $PM_{2.5}$ urban background levels, however stronger local contributions are expected considering urban traffic sites (where most critical PM exceedances in the Paris agglomeration occur) and/or PM_{10} (for which long-range transport is reduced by faster deposition).

Acknowledgements

This work is funded by a PhD DIM (*domaine d'intérêt majeur*) grant from the Ile-de-France region. The PARTICULES project has been funded by the French state, the Ile-de-France region and the Paris city. The authors gratefully acknowledge Jean-Charles Dupont and the SIRTA (sirta.ipsl.fr) for the useful boundary layer height data. Meteorological data have been kindly provided by METEO France.

References

AIRPARIF : Inventaire des émissions en Ile-de-France – Méthodologie et résultats – Année 2005 (in french), 2010.

AIRPARIF : Source apportionment of airborne particles in the Ile-de-France region, 2012.

Andreae, M. O. and Gelencsér, A. : Black carbon or brown carbon ? The nature of light-absorbing carbonaceous aerosols, Atmos. Chem. Phys., 6, 3131–3148, 2006.

Ansari, A. S. and Pandis, S. N. : Response of Inorganic PM to Precursor Concentrations, Environ. Sci. Technol., 32, 2706–2714, 1998.

Aumont, B., Chervier, F., and Laval, S. : Contribution of HONO sources to the NOx/HOx/O3 chemistry in the polluted boundary layer, Atmos. Environ., 37, 487–498, 2003.

Baumgardner, R. E., Lavery, T. F., Rogers, C. M., and Isil, S. S. : Estimates of the atmospheric deposition of sulfur and nitrogen species : Clean Air Status and Trends Network 1990-2000., Environ. Sci. Technol., 36, 2614–29, 2002.

Berge, E. : Coupling of wet scavenging of sulphur to clouds in a numerical weather prediction model, Tellus B, 45, 1–22, 1993.

Bergström, R., Denier van der Gon, H. A. C., Prévôt, A. S. H., Yttri, K. E., and Simpson, D. : Modelling of organic aerosols over Europe (2002-2007) using a volatility basis set (VBS) framework : application of different assumptions regarding the formation of secondary organic aerosol, Atmos. Chem. Phys., 12, 8499–8527, 2012.

Bessagnet, B., Menut, L., Curci, G., Hodzic, A., Guillaume, B., Liousse, C., Moukhtar, S., Pun, B., Seigneur, C., and Schulz, M. : Regional modeling of carbonaceous aerosols over Europe, focus on secondary organic aerosols, J. Atmos. Chem., 61, 175–202, 2009.

Bond, T. C., Doherty, S. J., Fahey, D. W., Forster, P. M., Berntsen, T., DeAngelo, B. J., Flanner, M. G., Ghan, S., Kärcher, B., Koch, D., Kinne, S., Kondo, Y., Quinn, P. K., Sarofim, M. C., Schultz, M. G., Schulz, M., Venkataraman, C., Zhang, H., Zhang, S., Bellouin, N., Guttikunda, S. K., Hopke, P. K., Jacobson, M. Z., Kaiser, J. W., Klimont,

Z., Lohmann, U., Schwarz, J. P., Shindell, D., Storelvmo, T., Warren, S. G., and Zender, C. S. : Bounding the role of black carbon in the climate system : A scientific assessment, J. Geophys. Res.-Atmos., 118, 1–173, 2013.

Boylan, J. W. and Russell, A. G. : PM and light extinction model performance metrics, goals, and criteria for three-dimensional air quality models, Atmos. Environ., 40, 4946–4959, 2006.

Bressi, M., Sciare, J., Ghersi, V., Bonnaire, N., Nicolas, J. B., Petit, J.-E., Moukhtar, S., Rosso, A., Mihalopoulos, N., and Féron, A.: A one-year comprehensive chemical characterisation of fine aerosol ($PM_{2.5}$) at urban, suburban and rural background sites in the region of Paris (France), Atmos. Chem. Phys., 13, 7825–7844, doi:10.5194/acp-13-7825-2013, 2013.

Carlton, A. G., Turpin, B. I., Altieri, K. E., Seitzinger, S. P., Mathur, R., Roselle, S. J., and Weber, R. J. : CMAQ model performance enhanced when in-cloud secondary organic aerosol is included : comparisons of organic carbon predictions with measurements., Environ. Sci. Technol., 42, 8798–802, 2008.

Cheng, Y.-H. and Tsai, C.-J. : Evaporation loss of ammonium nitrate particles during filter sampling, J. Aerosol Sci., 28, 1553–1567, 1997.

Chin, M., Rood, R. B., Lin, S.-J., Müller, J.-F., and Thompson, A. M. : Atmospheric sulfur cycle simulated in the global model GOCART : Model description and global properties, J. Geophys. Res., 105, 24,671-24,687, 2000.

Chow, J. C. : Health Effects of Fine Particulate Air Pollution : Lines that Connect, J. Air Waste Manage., 56, 707–708, 2006.

Cimini, N., Angelini, F., Dupont, J.-C., Pal, S., and Haeffelin, M. : Mixing layer height retrievals by multichannel microwave radiometer observations, Atmospheric Measurement Techniques, 6, 2941–2951, doi:10.5194/amt-6-2941-2013, 2013.

Couvidat, F., Debry, E., Sartelet, K., and Seigneur, C. : A hydrophilic/hydrophobic organic (H2O) aerosol model : Development, evaluation and sensitivity analysis, J. Geophys. Res., 117, D10 304, doi:10.1029/2011JD017214, 2012.

Couvidat, F., Kim, Y., Sartelet, K., Seigneur, C., Marchand, N., and Sciare, J. : Modeling secondary organic aerosol in an urban area : application to Paris, France, Atmos. Chem. Phys., 13, 983–996, 2013.

Crippa, M., DeCarlo, P. F., Slowik, J. G., Mohr, C., Heringa, M. F., Chirico, R., Poulain, L., Freutel, F., Sciare, J., Cozic, J., Di Marco, C. F., Elsasser, M., Nicolas, J. B., Marchand, N., Abidi, E., Wiedensohler, A., Drewnick, F., Schneider, J., Borrmann, S., Nemitz, E.,

Zimmermann, R., Jaffrezo, J.-L., Prévôt, A. S. H., and Baltensperger, U. : Wintertime aerosol chemical composition and source apportionment of the organic fraction in the metropolitan area of Paris, Atmos. Chem. Phys., 13, 961–981, 2013.

Donahue, N. M., Robinson, A. L., Stanier, C. O., and Pandis, S. N. : Coupled partitioning, dilution, and chemical aging of semivolatile organics., Environ. Sci. Technol., 40, 2635–43, 2006.

Dudhia, J. : A Nonhydrostatic Version of the Penn State-NCAR Mesoscale Model : Validation Tests and Simulation of an Atlantic Cyclone and Cold Front, Mon. Weather Rev., 121, 1493–1513, 1993.

EEA : CORINE land cover technical guide - Addendum 2000, Tech. Rep. 40, 2000.

EEA : Air quality in Europe - 2012 report, Tech. Rep. 4, EEA, 2012.

EEA : EMEP/EEA air pollutant emission inventory guidebook 2013, Tech. Rep. 12, EEA, 2013.

Ervens, B., Turpin, B. J., and Weber, R. J. : Secondary organic aerosol formation in cloud droplets and aqueous particles (aqSOA) : a review of laboratory, field and model studies, Atmos. Chem. Phys., 11, 11 069–11 102, 2011.

Favez, O., Cachier, H., Sciare, J., Sarda-Estève, R., and Martinon, L. : Evidence for a significant contribution of wood burning aerosols to PM2.5 during the winter season in Paris, France, Atmos. Environ., 43, 3640–3644, 2009.

Folberth, G. A., Hauglustaine, D. A., Lathière, J., and Brocheton, F. : Interactive chemistry in the Laboratoire de Météorologie Dynamique general circulation model : model description and impact analysis of biogenic hydrocarbons on tropospheric chemistry, Atmos. Chem. Phys., 6, 2273–2319, 2006.

Forster, P., Ramaswamy, V., Artaxo, P., Berntsen, T., Betts, R., Fahey, D.W., Haywood, J., Lean, J., Lowe, D.C., Myhre, G., Nganga, J., Prinn, R., Raga, G., Schulz, M., Van Dorland, R. : Changes in Atmospheric Constituents and in Radiative Forcing. In: Climate Change 2007: The Physical Science Basis. Contribution of Working Group I to the Fourth Assessment Report of the Intergovernmental Panel on Climate Change [Solomon, S., D. Qin, M. Manning, Z. Chen, M. Marquis, K.B. Averyt, M.Tignor and H.L. Miller (eds.)]. Cambridge University Press, Cambridge, United Kingdom and New York, NY, USA, 2007.

Gelbard, F. and Seinfeld, J. H. : Simulation of multicomponent aerosol dynamics, J. Colloid Interf. Sci., 78, 485–501, 1980.

Guelle, W., Balkanski, Y. J., Dibb, J. E., Schulz, M., and Dulac, F. : Wet deposition in a global size-dependent aerosol transport model : 2. Influence of the scavenging scheme on 210 Pb vertical profiles, surface concentrations, and deposition, J. Geophys. Res., 103, 28,875-28,891, 1998.

Guenther, A., Karl, T., Harley, P., Wiedinmyer, C., Palmer, P. I., and Geron, C. : Estimates of global terrestrial isoprene emissions using MEGAN (Model of Emissions of Gases and Aerosols from Nature), Atmos. Chem. Phys., 6, 3181–3210, 2006.

Haeffelin, M., Angelini, F., Morille, Y., Martucci, G., Frey, S., Gobbi, G. P., Lolli, S., O"Dowd, C. D., Sauvage, L., Xueref-Rémy, I., Wastine, B., and Feist, D. G. : Evaluation of Mixing-Height Retrievals from Automatic Profiling Lidars and Ceilometers in View of Future Integrated Networks in Europe, Bound.-Lay. Meteorol., 143, 49–75, 2011.

Hallquist, M., Wenger, J. C., Baltensperger, U., Rudich, Y., Simpson, D., Claeys, M., Dommen, J., Donahue, N. M., George, C., Goldstein, A. H., Hamilton, J. F., Herrmann, H., Hoffmann, T., Iinuma, Y., Jang, M., Jenkin, M. E., Jimenez, J. L., Kiendler-Scharr, A., Maenhaut, W., McFiggans, G., Mentel, T. F., Monod, A., Prévôt, A. S. H., Seinfeld, J. H., Surratt, J. D., Szmigielski, R., and Wildt, J. : The formation, properties and impact of secondary organic aerosol : current and emerging issues, Atmos. Chem. Phys., 9, 5155–5236, 2009.

Healy, R. M., Sciare, J., Poulain, L., Kamili, K., Merkel, M., Müller, T., Wiedensohler, A., Eckhardt, S., Stohl, A., Sarda-Estève, R., McGillicuddy, E., O'Connor, I. P., Sodeau, J. R., and Wenger, J. C. : Sources and mixing state of size-resolved elemental carbon particles in a European megacity : Paris, Atmos. Chem. Phys., 12, 1681–1700, 2012.

Hering, S. and Cass, G. : The magnitude of bias in the measurement of PM25 arising from volatilization of particulate nitrate from Teflon filters, J. Air Waste Manage., 49, 725–733, 1999.

Hodzic, A., Vautard, R., Bessagnet, B., Lattuati, M., and Moreto, F. : Long-term urban aerosol simulation versus routine particulate matter observations, Atmos. Environ., 39, 5851–5864, 2005.

Hoffman, M. R. and Calvert, J. G. : Chemical transformation modules for eulerian acid deposition models,. EPA/600/3-85/017, 1985.

Hu, Y., Odman, M. T., and Russell, A. G. : Top-down analysis of the elemental carbon emissions inventory in the United States by inverse modeling using Community Multiscale Air Quality model with decoupled direct method (CMAQ-DDM), J. Geophys. Res., 114, D24302, doi: 10.1029/2009JD011987, 2009.

Huffman, J. A., Docherty, K. S., Aiken, A. C., Cubison, M. J., Ulbrich, I. M., DeCarlo, P. F., Sueper, D., Jayne, J. T., Worsnop, D. R., Ziemann, P. J., and Jimenez, J. L. : Chemically-resolved aerosol volatility measurements from two megacity field studies, Atmos. Chem. Phys., 9, 7161–7182, 2009.

Jacob, D. J. : Heterogeneous chemistry and tropospheric ozone, Atmos. Environ., 34, 2131–2159, 2000.

Kai, Z., Yuesi, W., Tianxue, W., Yousef, M., and Frank, M. : Properties of nitrate, sulfate and ammonium in typical polluted atmospheric aerosols (PM_{10}) in Beijing, Atmos. Res., 84, 67–77, 2007.

Kalberer, M., Henne, S., Prevot, A., and Steinbacher, M. : Vertical transport and degradation of polycyclic aromatic hydrocarbons in an Alpine Valley, Atmos. Environ., 38, 6447–6456, 2004.

Keck, L. and Wittmaack, K. : Effect of filter type and temperature on volatilisation losses from ammonium salts in aerosol matter, Atmos. Environ., 39, 4093–4100, 2005.

Konovalov, I. B., Beekmann, M., Richter, A., and Burrows, J. P. : Inverse modelling of the spatial distribution of NO_x emissions on a continental scale using satellite data, Atmos. Chem. Phys., 6, 1747–1770, 2006.

Kulmala, M., Laaksonen, A., and Pirjola, L. : Parameterizations for sulfuric acid/water nucleation rates, J. Geophys. Res., 103, 8301-8307, 1998.

Lac, C., Donnelly, R. P., Masson, V., Pal, S., Riette, S., Donier, S., Queguiner, S., Tanguy, G., Ammoura, L., and Xueref-Rem, I. : CO_2 dispersion modelling over Paris region within the CO_2-MEGAPARIS project, Atmos. Chem. Phys., 13, 4941–4961, doi:10.5194/acp-13-4941-2013, 2013.

Lane, T. E., Donahue, N. M., and Pandis, S. N. : Simulating secondary organic aerosol formation using the volatility basis-set approach in a chemical transport model, Atmos. Environ., 42, 7439–7451, 2008.

Lee, Y. N. and Schwartz, S. E. : Precipitation scavenging, dry deposition and resuspension, vol. 1., chapter Kinetics of oxidation of aqueous sulfur (IV) by nitrogen dioxide. Elsevier, New York, 453-470, 1983.

Lenschow, P., Abraham, H.-J., Kutzner, K., Lutz, M., Preub, J.-D., and Reichenbächer, W. : Some ideas about the sources of PM_{10}, Atmos. Environ., 35, 23–33, 2001.

Likens, G. E., Driscoll, C. T., and Buso, D. C. : Long-term effects of acid rain : response and recovery of a forest ecosystem, Science, 272, 244–246, 1996.

Lohmann, U. and Feichter, J. : Global indirect aerosol effects : a review, Atmos. Chem. Phys., 5, 715–737, 2005.

Lombardo, T., Gentaz, L., Verney-Carron, A., Chabas, A., Loisel, C., Neff, D., and Leroy, E. : Characterisation of complex alteration layers in medieval glasses, Corros. Sci., 72, 10–19, 2013.

Menut, L., Bessagnet, B., Colette, A., and Khvorostiyanov, D. : On the impact of the vertical resolution on chemistry-transport modelling, Atmos. Environ., 67, 370–384, 2013.

Milford, C., Castell, N., Marrero, C., Rodríguez, S., Sánchez de la Campa, A. M., Fernández-Camacho, R., de la Rosa, J., and Stein, A. F. : Measurements and simulation of speciated $PM_{2.5}$ in south-west Europe, Atmos. Environ., 77, 36–50, 2013.

Murphy, B. N. and Pandis, S. N. : Simulating the formation of semivolatile primary and secondary organic aerosol in a regional chemical transport model., Environ. Sci. Technol., 43, 4722–8, 2009.

Nenes, A., Pandis, S., and Pilinis, C. : ISORROPIA : A New Thermodynamic Equilibrium Model for Multiphase Multicomponent Inorganic Aerosols, Aquat. Geochem., 4, 123–152, 1998.

Nopmongcol, U., Koo, B., Tai, E., Jung, J., Piyachaturawat, P., Emery, C., Yarwood, G., Pirovano, G., Mitsakou, C., and Kallos, G. : Modeling Europe with CAMx for the Air Quality Model Evaluation International Initiative (AQMEII), Atmos. Environ., 53, 177–185, 2012.

Nussbaumer, T., Czasch, C., Klippel, N., Johansson, L., and Tullin, C. : Particulate emissions from biomass combustion in IEA countries, survey on measurements and emission factors, Tech. Rep. January, 2008.

Pal, S., Xueref-Remy, I., Ammoura, L., Chazette, P., Gibert, F., Royer, P., Dieudonné, E., Dupont, J.-C., Haeffelin, M., Lac, C., Lopez, M., Morille, Y., and Ravetta, F. : Spatio-temporal variability of the atmospheric boundary layer depth over the Paris agglomeration : An assessment of the impact of the urban heat island intensity, Atmos. Environ., 63, 261–275, 2012.

Pal, S., Haeffelin, M., and Batchvarova, E. : Exploring a geophysical process-based attribution technique for the determination of the atmospheric boundary layer depth using aerosol lidar and near-surface meteorological measurements, in press, J. Geophys. Res.-Atmos., 118, 1–19, doi:10.1002/jgrd.50710, 2013.

Pang, Y., Eatough, N. L., Wilson, J., and Eatough, D. J. : Effect of semivolatile material on $PM_{2.5}$ measurement by the $PM_{2.5}$ Federal reference method sampler at Bakersfield, California, Aerosol Sci. Tech., 36, 289–299, 2002.

Pankow, J. F. : An absorption model of gas/aerosol partition involved in the formation of secondary organic aerosol. Atmos. Environ., 28, 189–193, 1994.

Pay, M. T., Jiménez-Guerrero, P., and Baldasano, J. M. : Assessing sensitivity regimes of secondary inorganic aerosol formation in Europe with the CALIOPE-EU modeling system, Atmos. Environ., 51, 146–164, 2012.

Pinder, R. W., Dennis, R. L., and Bhave, P. V. : Observable indicators of the sensitivity of $PM_{2.5}$ nitrate to emission reductions - Part I : Derivation of the adjusted gas ratio and applicability at regulatory-relevant time scales, Atmos. Environ., 42, 1275–1286, 2008.

Pun, B. K. and Seigneur, C. : Investigative modeling of new pathways for secondary organic aerosol formation, Atmos. Chem. Phys., 7, 2199–2216, 2007.

Rao, S. T., Galmarini, S., and Puckett, K. : Air Quality Model Evaluation International Initiative (AQMEII) : Advancing the state of the science in regional photochemical modeling and its applications, B. Am. Meteorol. Soc., 92, 23–30, 2011.

Rengarajan, R., Sudheer, A. K., and Sarin, M. M. : Wintertime $PM_{2.5}$ and PM_{10} carbonaceous and inorganic constituents from urban site in western India, Atmos. Res., 102, 420–431, 2011.

Robinson, A. L., Donahue, N. M., Shrivastava, M. K., Weitkamp, E. A., Sage, A. M., Grieshop, A. P., Lane, T. E., Pierce, J. R., and Pandis, S. N. : Rethinking organic aerosols : semivolatile emissions and photochemical aging., Science (New York, N.Y.), 315, 1259–62, 2007.

Salako, G. O. : Exploring the variation between EC and BC in a variety of locations, Aerosol Air Qual. Res., 12, 1–7, 2012.

Sartelet, K., Debry, E., Fahey, K., Roustan, Y., Tombette, M., and Sportisse, B. : Simulation of aerosols and gas-phase species over Europe with the Polyphemus system : Part I - Model-to-data comparison for 2001, Atmos. Environ., 41, 6116–6131, 2007.

Schmidt, H. and Derognat, C. : A comparison of simulated and observed ozone mixing ratios for the summer of 1998 in Western Europe, Atmos. Environ., 35, 6277–6297, 2001.

Sciare, J., D'Argouges, O., Zhang, Q. J., Sarda-Estève, R., Gaimoz, C., Gros, V., Beekmann, M., and Sanchez, O. : Comparison between simulated and observed chemical composition of fine aerosols in Paris (France) during springtime : contribution of regional versus continental emissions, Atmos. Chem. Phys., 10, 11 987–12 004, 2010.

Sciare, J., D'Argouges, O., Sarda-Estève, R., Gaimoz, C., Dolgorouky, C., Bonnaire, N., Favez, O., Bonsang, B., and Gros, V. : Large contribution of water-insoluble secondary organic aerosols in the region of Paris (France) during wintertime, J. Geophys. Res., 116, D22 203, doi:10.1029/2011JD015756, 2011.

Seinfeld, J. H., Pandis, S. N. : Atmospheric chemistry and physics : from air pollution to climate change. Wiley-Interscience, 2006.

Solazzo, E., Bianconi, R., Pirovano, G., Matthias, V., Vautard, R., Moran, M. D., Wyat Appel, K., Bessagnet, B., Brandt, J. r., Christensen, J. H., Chemel, C., Coll, I., Ferreira, J., Forkel, R., Francis, X. V., Grell, G., Grossi, P., Hansen, A. B., Miranda, A. I., Nopmongcol, U., Prank, M., Sartelet, K. N., Schaap, M., Silver, J. D., Sokhi, R. S., Vira, J., Werhahn, J., Wolke, R., Yarwood, G., Zhang, J., Rao, S. T., and Galmarini, S. : Operational model evaluation for particulate matter in Europe and North America in the context of AQMEII, Atmos. Environ., 53, 75–92, 2012.

Stern, R., Builtjes, P., Schaap, M., Timmermans, R., Vautard, R., Hodzic, A., Memmesheimer, M., Feldmann, H., Renner, E., and Wolke, R. : A model inter-comparison study focussing on episodes with elevated PM_{10} concentrations, Atmos. Environ., 42, 4567–4588, 2008.

Stohl, A., Haimberger, L., Scheele, M. P., and Wernli, H. : An intercomparison of results from three trajectory models, Meteorol. Appl., 8, 127–135, 2001.

Sun, Y.-L., Zhang, Q., Schwab, J. J., Demerjian, K. L., Chen, W.-N., Bae, M.-S., Hung, H.-M., Hogrefe, O., Frank, B., Rattigan, O. V., and Lin, Y.-C. : Characterization of the sources and processes of organic and inorganic aerosols in New York city with a high-resolution time-of-flight aerosol mass apectrometer, Atmos. Chem. Phys., 11, 1581–1602, 2011.

Tsyro, S. : First estimates of the effect of aerosol dynamics in the calculation of PM_{10} and $PM_{2.5}$, EMEP report, 2002.

Valari, M. and Menut, L. : Does an increase in Air Quality models resolution bring surface ozone concentrations closer to reality ?, J. Atmos. Ocean. Tech., 25, 1955–1968, 2008.

Van Dingenen, R., Raes, F., Putaud, J.-P., Baltensperger, U., Charron, A., Facchini, M.-C., Decesari, S., Fuzzi, S., Gehrig, R., Hansson, H.-C., Harrison, R. M., Hüglin, C., Jones, A. M., La j, P., Lorbeer, G., Maenhaut, W., Palmgren, F., Querol, X., Rodriguez, S., Schneider, J., Brink, H. T., Tunved, P., Tørseth, K., Wehner, B., Weingartner, E., Wiedensohler, A., and Wåhlin, P. : A European aerosol phenomenology - 1 : physical characteristics of particulate matter at kerbside, urban, rural and background sites in Europe, Atmos. Environ., 38, 2561–2577, 2004.

Vautard, R., Moran, M. D., Solazzo, E., Gilliam, R. C., Matthias, V., Bianconi, R., Chemel, C., Ferreira, J., Geyer, B., Hansen, A. B., Jericevic, A., Prank, M., Segers, A., Silver, J. D., Werhahn, J., Wolke, R., Rao, S., and Galmarini, S. : Evaluation of the meteorological forcing used for the Air Quality Model Evaluation International Initiative (AQMEII) air quality simulations, Atmos. Environ., 53, 15–37, 2012.

Vestreng, V. : Inventory Review 2007, 6079, 2007.

Wesely, M. : Parameterization of surface resistances to gaseous dry deposition in regional-scale numerical models, Atmos. Environ., 23, 1293–1304, 1989.

Yu, X., Lee, T., Ayres, B., Kreidenweis, S., Malm, W., and Collett Jr, L. : Loss of fine particle ammonium from denuded nylon filters, Atmos. Environ., 40, 4797–4807, 2006.

Zhang, Q. J., Beekmann, M., Drewnick, F., Freutel, F., Schneider, J., Crippa, M., Prevot, A. S. H., Baltensperger, U., Poulain, L., Wiedensohler, A., Sciare, J., Gros, V., Borbon, A., Colomb, A., Michoud, V., Doussin, J.-F., Denier van der Gon, H. A. C., Haeffelin, M., Dupont, J.-C., Siour, G., Petetin, H., Bessagnet, B., Pandis, S. N., Hodzic, A., Sanchez, O., Honoré, C., and Perrussel, O. : Formation of organic aerosol in the Paris region during the MEGAPOLI summer campaign : evaluation of the volatility-basis-set approach within the CHIMERE model, Atmos. Chem. Phys., 13, 5767–5790, 2013.

Table 1: Measurement techniques and instruments for $PM_{2.5}$ and each of its compounds.

Species	Measurement technique	Instrument	Uncertainty/ Sensitivity
$PM_{2.5}$	Gravimetry	Microbalance Sartorius MC21S	- / ± 1 µg
	TEOM-FDMS		
Organic carbon (OC), elemental carbon (EC)	Thermo-optical	Sunset Laboratory instrument, EUSAAR-2 protocol	20%[1] 20%
Ions (NO_3^-, SO_4^{2-}, NH_4^+)	Ion chromatography	Dionex DX600	5%[1]

(1) measurement error, not including filter sampling errors

Table 2: Domains description.

Domain name	Cells number (SW corner location)	Resolution
LAR	67x46 (-10.5°; 35°)	~50 x 50 km (0.5 x 0.5°)
MED	68x56 (-5.19°; 45.05°)	15 x 15 km
FIN	150x186 (-0.01°; 46.17°)	3 x 3 km

1 Table 3: Mean absolute and relative uncertainties on observed imported and local
2 contributions at three time scales (see text for details), and range of uncertainties among
3 all monthly contributions over the period.

Contribution	Species	Absolute (μg m^{-3}) and relative (%) uncertainty					
		Daily mean		Monthly mean range		Yearly mean	
Advected	$PM_{2.5}$	4.40	44%	(0.37, 1.88)	(5%, 18%)	0.32	3%
	EC	0.30	87%	(0.04, 0.12)	(11%, 25%)	0.02	5%
	OM	2.77	69%	(0.20, 1.27)	(7%, 30%)	0.21	5%
	Ammonium	0.48	49%	(0.04, 0.33)	(6%, 21%)	0.04	3%
	Nitrate	1.15	>100%	(0.12, 0.57)	(11%, 35%)	0.10	5%
	Sulfate	0.59	43%	(0.08, 0.28)	(5%, 14%)	0.04	2%
Local	$PM_{2.5}$	7.13	>100%	(0.77, 2.32)	(27%, 66%)	0.46	11%
	EC	*	37%	*	(4%, 11%)	*	2%
	OM	*	>100%	*	(15%, 93%)	*	13%
	Ammonium	*	>100%	*	(18%, >100%)	*	24%
	Nitrate	*	>100%	*	(16%, >100%)	*	17%
	Sulfate	*	>100%	*	(26%, >100%)	*	38%

4 * Idem than advected.

5
6

1 Table 4: Statistical results for meteorological parameters simulation.

Paris, MONTSOURIS site	MB	NMB (%)	RMSE	NRMSE (%)	R
Temperature (°C)	-1.0	-	1.6	-	0.99
Wind speed (m s^{-1})	+0.1	+2.3	0.9	30	0.78
Relative humidity (%)	+3.1	+4.4	9.3	13	0.88
Precipitations (mm h^{-1})	-0.0	-33.7	0.6	856	0.19
Boundary layer height (m)	+223.8	+37.8	522.8	88	0.61

2

3

Table 5: Average and standard deviation of the advected and local observed $PM_{2.5}$ contribution ($\mu g\ m^{-3}$), depending on the air mass origin.

Air mass origin		All	RNE	RUS	RNW
Rural contribution	Mean	11.3	17.6	8.5	8.6
	Standard deviation	9.0	11.5	5.4	6.2
Urban contribution	Mean	4.0	3.7	6.1	3.0
	Standard deviation	3.6	3.0	4.2	3.0

Table 6: Observed yearly advected and local relative contributions to urban background $PM_{2.5}$ (and its major chemical constituents) in Paris.

	Contribution to $PM_{2.5}$ (%)	$PM_{2.5}$ compound contribution (%)	
Advected	71.2	EC	3.0
		OM	29
		Nitrate	11
		Sulfate	12
		Ammonium	7.0
Local	28.8	EC	8.4
		OM	13
		Nitrate	3.0
		Sulfate	0.5
		Ammonium	0.8

Table 7: Statistical results for local and advected contribution and urban background concentration (see metrics definitions in Sect. 4.2, N is the number of daily data).

	Chemical constituent	MB ($\mu g\ m^{-3}$)	NMB (%)	RMSE ($\mu g\ m^{-3}$)	NRMSE (%)	R	N
Local contribution	$PM_{2.5}$	+2.0	+51	4.71	117	0.41	333
	EC	+1.1	+103	1.50	146	0.45	321
	OM	+1.3	+76	2.55	157	0.23	332
	Ammonium	-0.18	-105	0.53	313	0.27	322
	Nitrate	-0.66	-109	1.44	240	0.31	322
	Sulfate	+0.04	+32	0.59	531	0.11	322
Advected contribution	$PM_{2.5}$	+0.13	+1.1	7.41	65	0.58	359
	EC	-0.07	-18	0.23	57	0.45	346
	OM	-2.6	-59	4.07	92	0.33	358
	Ammonium	+0.36	+30	1.04	87	0.70	347
	Nitrate	+1.4	+63	2.74	127	0.73	347
	Sulfate	-0.30	-17	1.34	75	0.48	347
Paris concentration	$PM_{2.5}$	+2.4	+16	8.47	56	0.59	336
	EC	+1.0	+70	1.50	104	0.54	336
	OM	-1.3	-21	3.33	56	0.48	336
	Ammonium	+0.15	+10	1.10	77	0.71	336
	Nitrate	+0.68	+23	2.44	84	0.80	336
	Sulfate	-0.34	-17	1.56	79	0.39	336

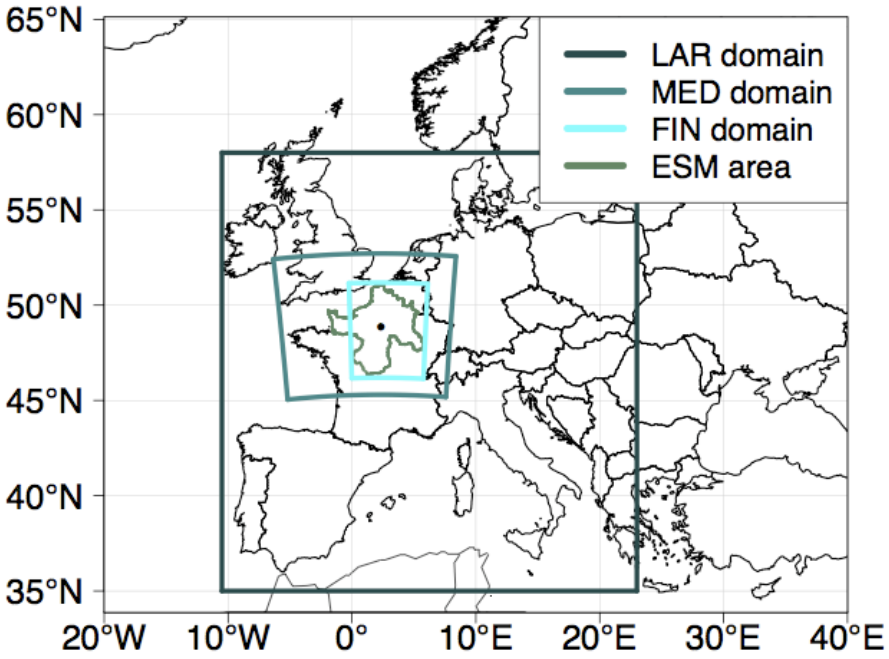

Figure 1: Nested domains used for the simulations, and ESM area of the bottom-up anthropogenic emission inventory.

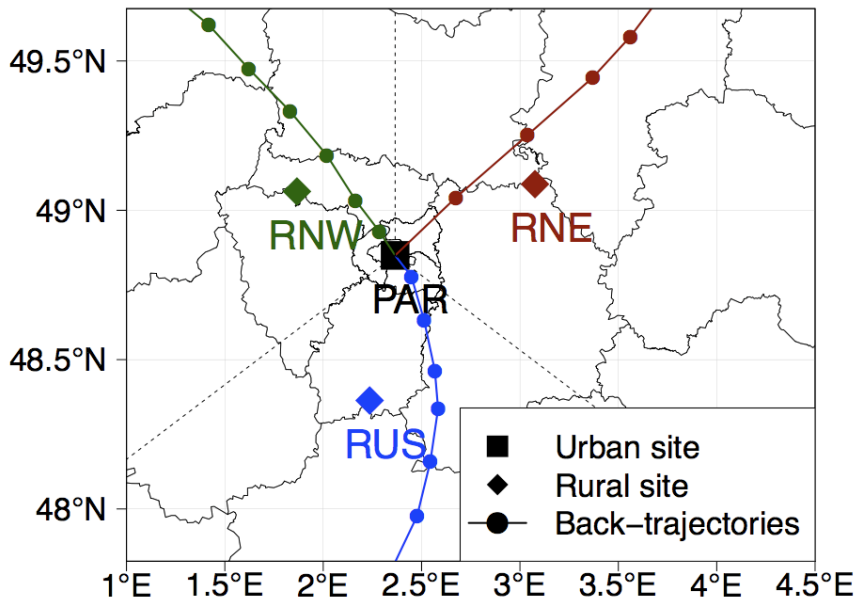

Figure 2: Location of measurement sites in Paris (urban site, PAR) and around (rural sites, RNE, RUS, RNW) the Greater Paris. Straight black lines delimit the three wind sectors. Back-trajectories for three specific days, one for each sector, are also represented by colored lines. Colored points over back-trajectories indicate air mass location at each hour.

1

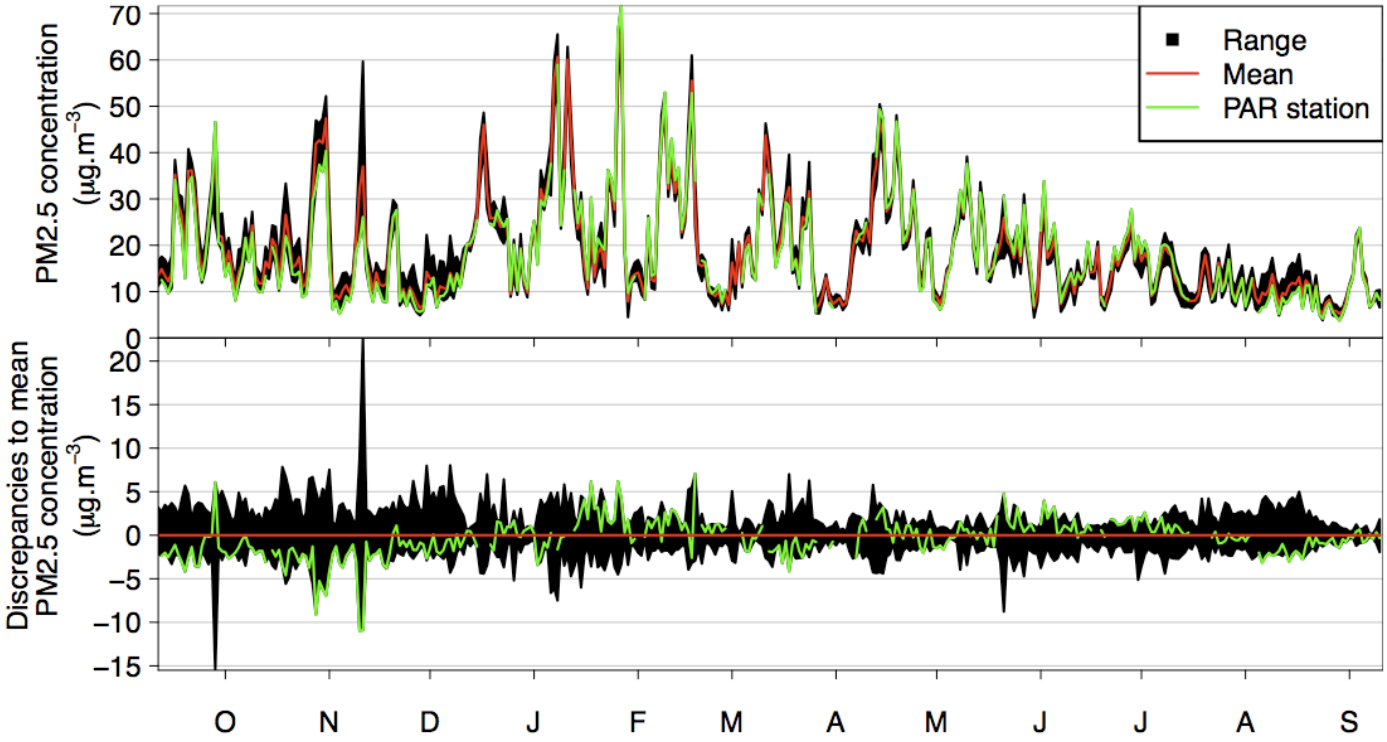

3 Figure 3: Daily $PM_{2.5}$ concentration range (black) from a set of four urban background
4 stations in the Greater Paris (top panel), with mean daily (red) and PAR (green)
5 concentration. Bottom panel: the same minus the mean $PM_{2.5}$ concentration.

6

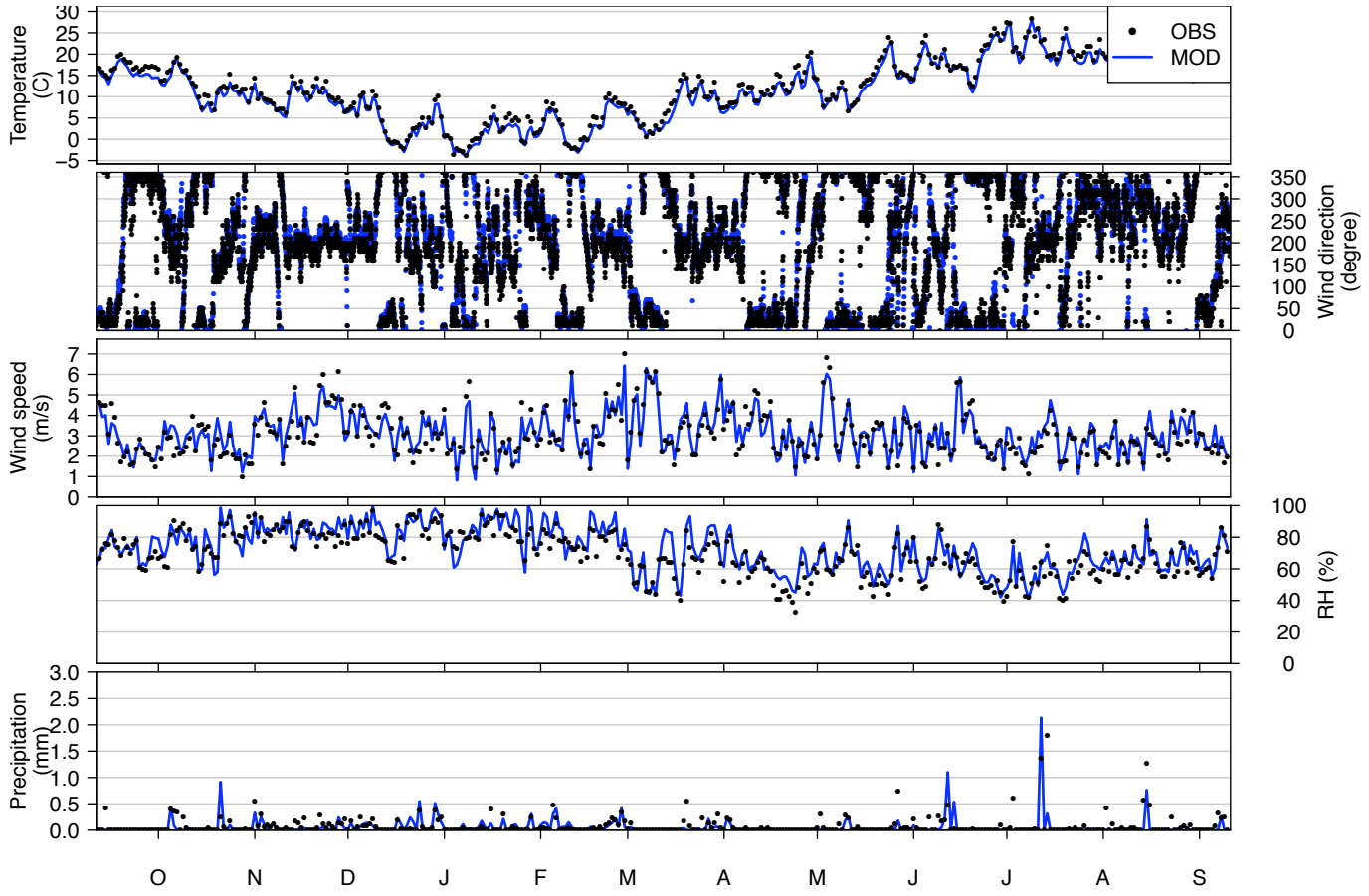

Figure 4: Measured and simulated meteorological parameters at the MONTSOURIS station (in the center of Paris). Temperature, wind speed, relative humidity (RH) and precipitations are reported as daily values while wind direction has a 1-h time resolution.

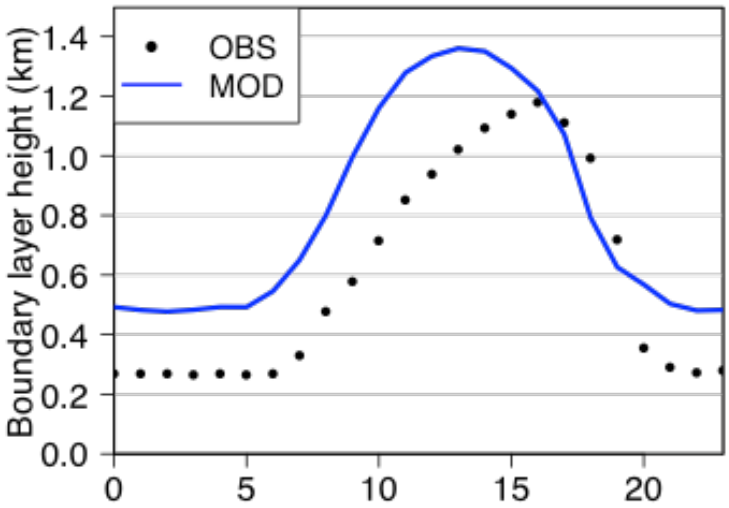

Figure 5: Boundary layer height diurnal profile at SIRTA station, measured (in black) and simulated (in blue) during the PARTICULES campaign .

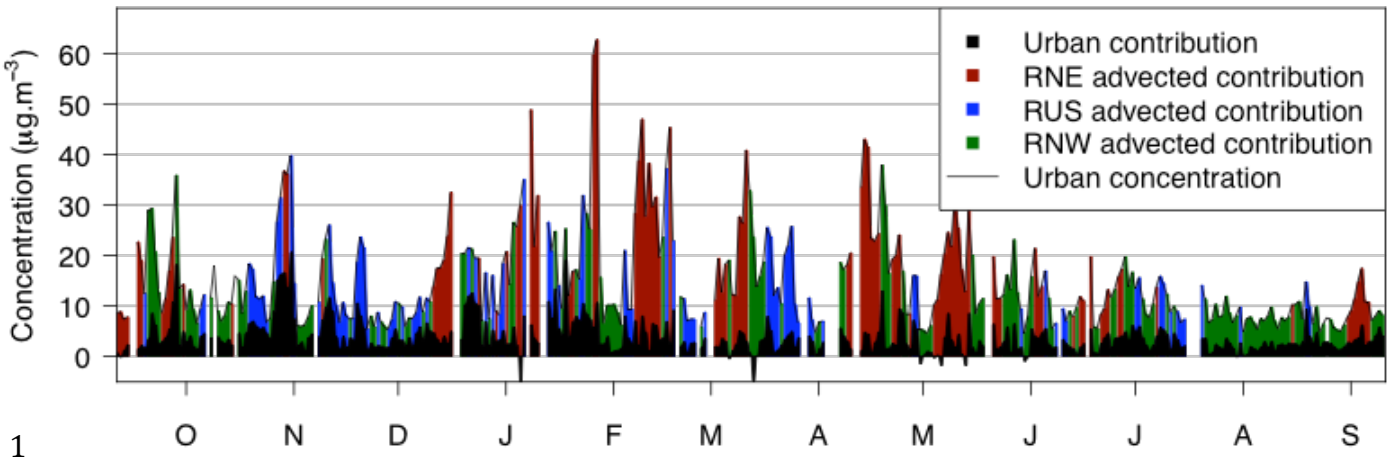

Figure 6: Imported and local contributions to the daily observed $PM_{2.5}$ concentrations in Paris (PAR). The urban local contribution is colored in black. Advected contributions are represented according to air mass origin in red (for north-east regime), blue (south) and green (north-west). Note that for several days, no chemical $PM_{2.5}$ speciation is available.

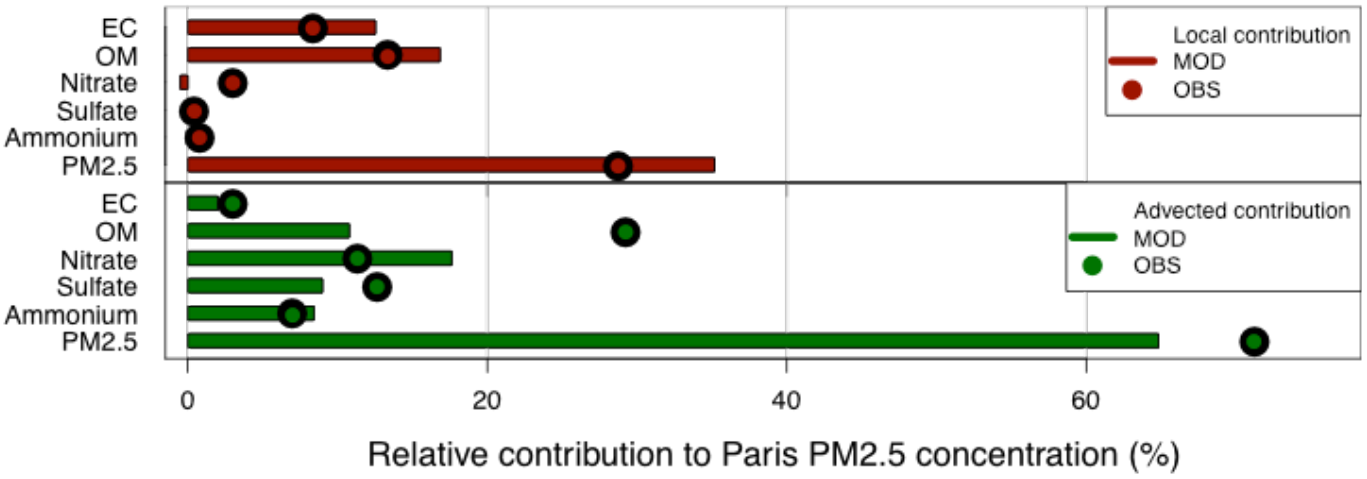

Figure 7: Mean relative local (top, red) and advected (bottom, green) contributions to the Greater Paris $PM_{2.5}$ urban background, for CHIMERE (bars) and observations (rounds). Note: These average values are based on the sub-period with a complete data set for all of the compounds (87% of the period).

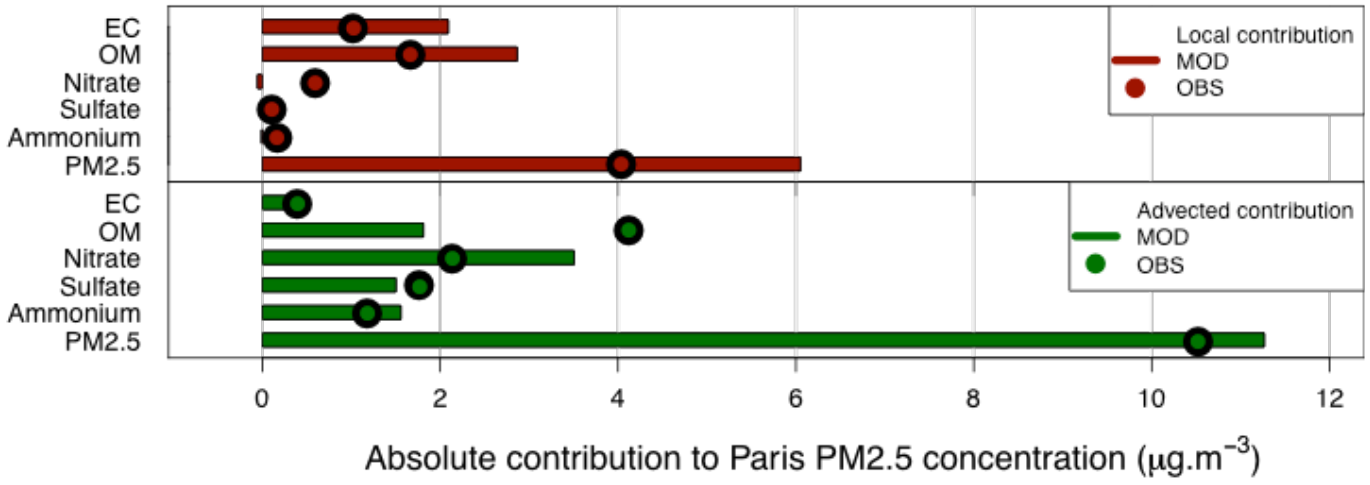

Figure 8: Same as Fig. 7, with absolute contributions.

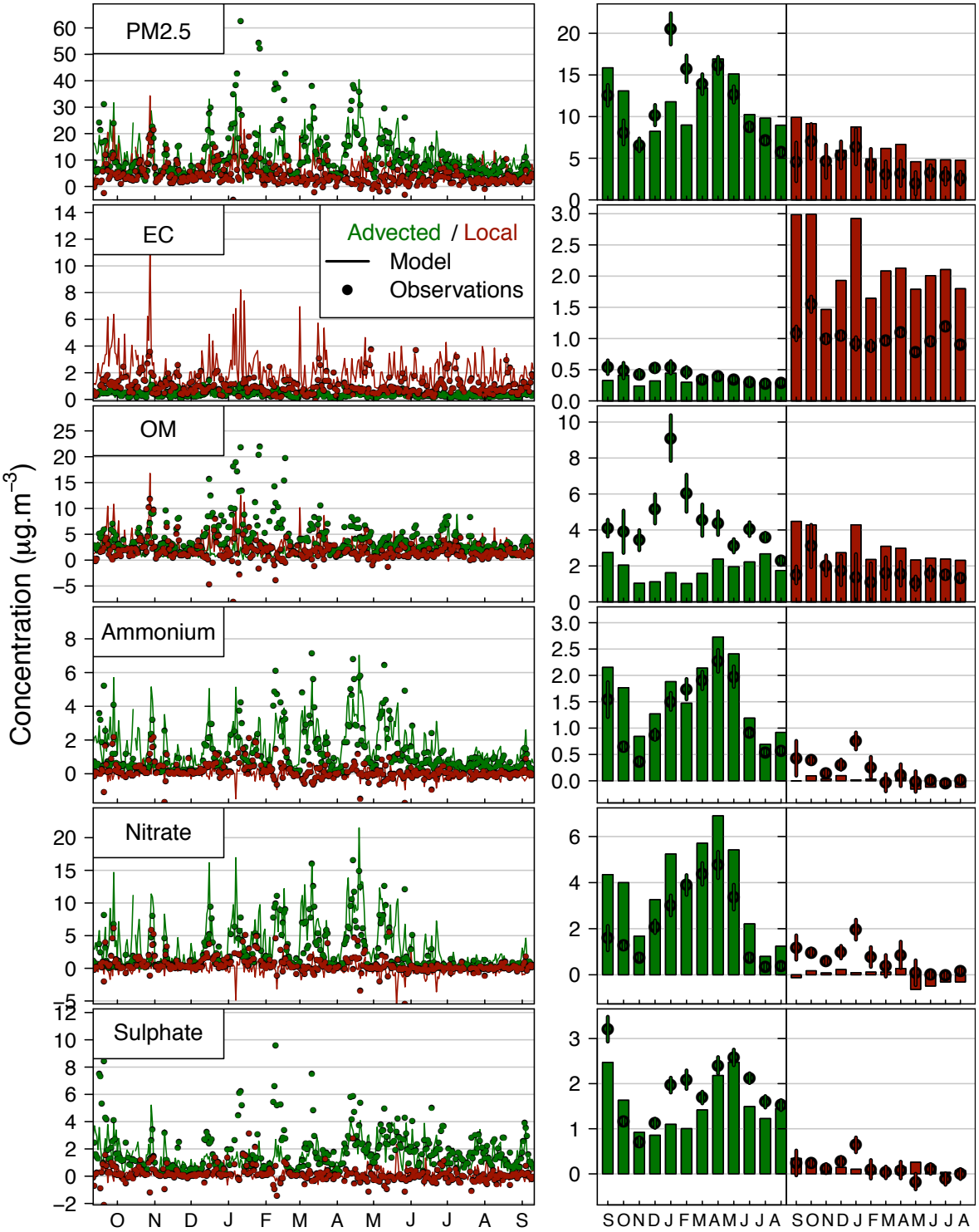

Figure 9: Daily time series (left panel) and monthly variations (right panel) of modeled (lines) and observed (points) advected (green) and local (red) contributions.

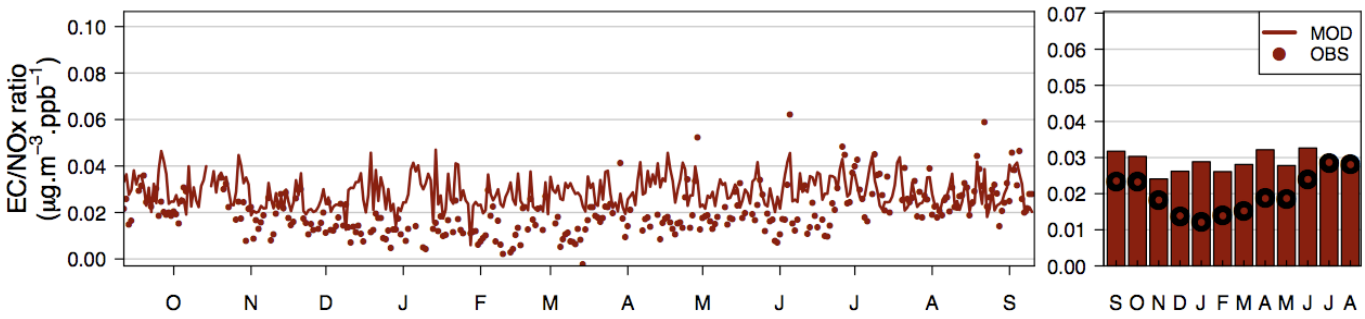

Figure 10: Local EC/NO_x ratio time series (left) and monthly averages (right) for model (line and bar) and observations (points).

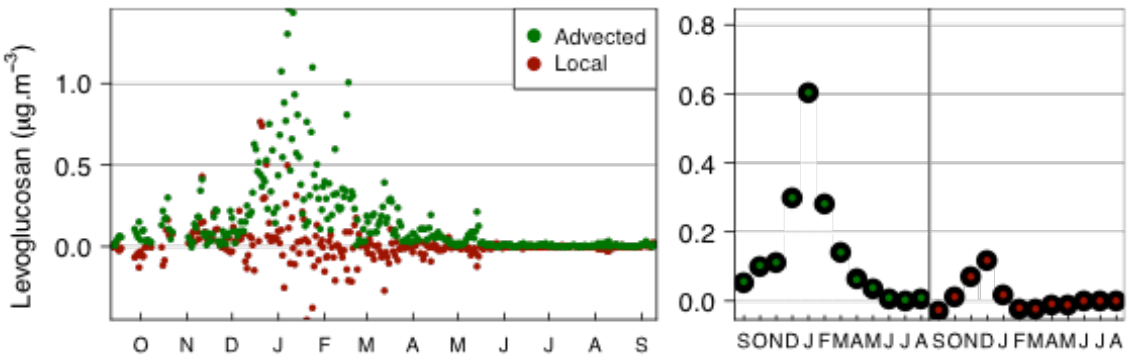

Figure 11: Daily (left panel) and monthly (right panel) advected (green) and local (red) levoglucosan contributions.

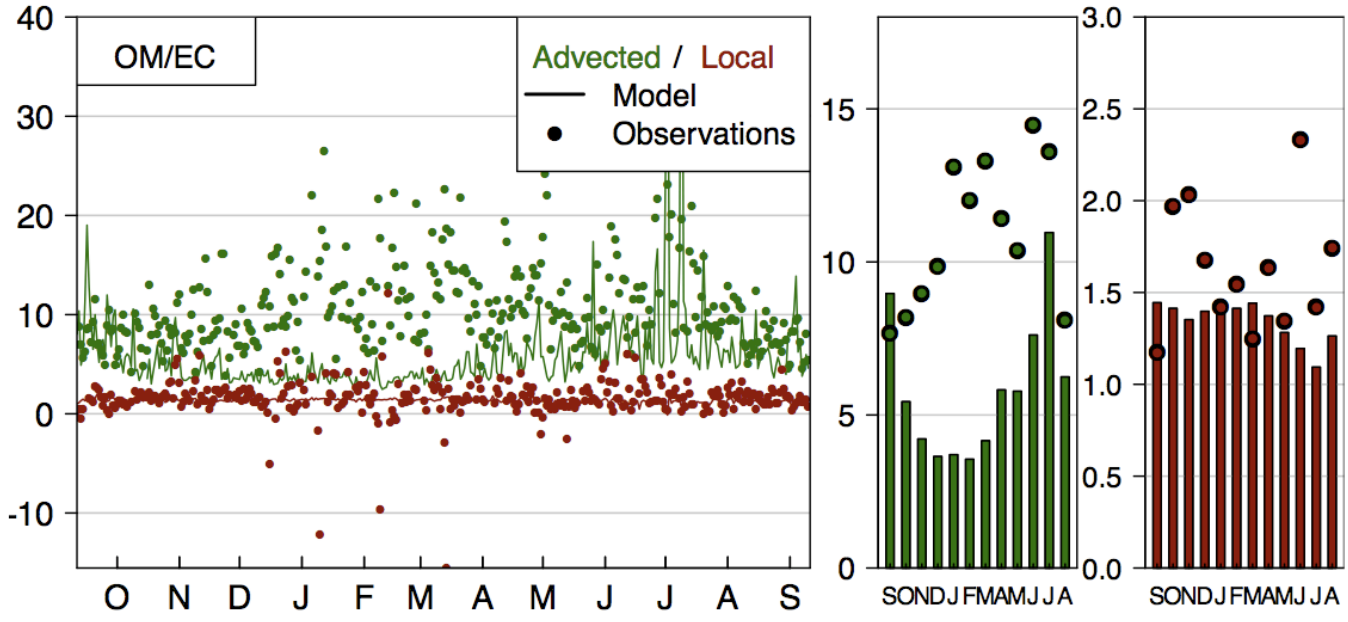

Figure 12: Local OM/EC ratio (unitless) time series (left) and monthly averages (right) for model (line and bars) and observations (points).

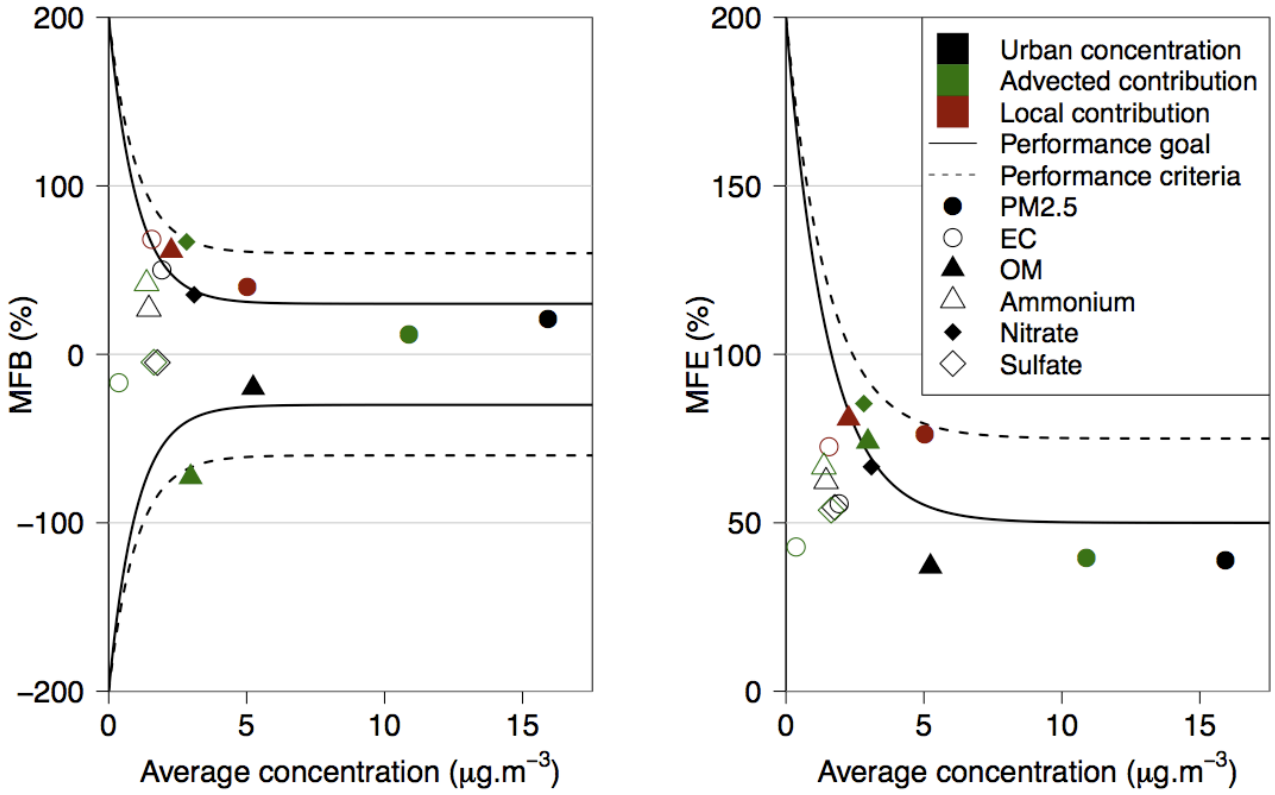

Figure 13: Mean fractional bias (left panel) and mean fractional error (right panel) depending on the average concentration defined as the average of the mean observed and the mean simulated concentration. Urban background concentrations, advected and local contributions of $PM_{2.5}$ and all its compounds are reported, as well as performance criteria (dotted line) and goal (continuous line). Secondary inorganics local contributions are not reported on the graph (see text).